

Winter 1988

The role of histidine in the mechanism of iron release from human serum transferrin

Donna M. Martin

University of New Hampshire, Durham

Follow this and additional works at: <https://scholars.unh.edu/dissertation>

Recommended Citation

Martin, Donna M., "The role of histidine in the mechanism of iron release from human serum transferrin" (1988). *Doctoral Dissertations*. 1563.

<https://scholars.unh.edu/dissertation/1563>

This Dissertation is brought to you for free and open access by the Student Scholarship at University of New Hampshire Scholars' Repository. It has been accepted for inclusion in Doctoral Dissertations by an authorized administrator of University of New Hampshire Scholars' Repository. For more information, please contact nicole.hentz@unh.edu.

INFORMATION TO USERS

The most advanced technology has been used to photograph and reproduce this manuscript from the microfilm master. UMI films the text directly from the original or copy submitted. Thus, some thesis and dissertation copies are in typewriter face, while others may be from any type of computer printer.

The quality of this reproduction is dependent upon the quality of the copy submitted. Broken or indistinct print, colored or poor quality illustrations and photographs, print bleedthrough, substandard margins, and improper alignment can adversely affect reproduction.

In the unlikely event that the author did not send UMI a complete manuscript and there are missing pages, these will be noted. Also, if unauthorized copyright material had to be removed, a note will indicate the deletion.

Oversize materials (e.g., maps, drawings, charts) are reproduced by sectioning the original, beginning at the upper left-hand corner and continuing from left to right in equal sections with small overlaps. Each original is also photographed in one exposure and is included in reduced form at the back of the book. These are also available as one exposure on a standard 35mm slide or as a 17" x 23" black and white photographic print for an additional charge.

Photographs included in the original manuscript have been reproduced xerographically in this copy. Higher quality 6" x 9" black and white photographic prints are available for any photographs or illustrations appearing in this copy for an additional charge. Contact UMI directly to order.

U·M·I

University Microfilms International
A Bell & Howell Information Company
300 North Zeeb Road, Ann Arbor, MI 48106-1346 USA
313/761-4700 800/521-0600

Order Number 8907445

**The role of histidine in the mechanism of iron release from
human serum transferrin**

Martin, Donna M., Ph.D.

University of New Hampshire, 1988

U·M·I

**300 N. Zeeb Rd.
Ann Arbor, MI 48106**

THE ROLE OF HISTIDINE IN THE MECHANISM
OF IRON RELEASE FROM HUMAN SERUM TRANSFERRIN

BY

DONNA M. MARTIN

BS, Salem State College, 1983

A Dissertation

Submitted to the University of New Hampshire
in Partial Fulfillment of the
Requirements for the Degree of

Doctor of Philosophy

in

Chemistry

December, 1988

This dissertation has been examined and approved.

N. Dennis Chasteen

N. Dennis Chasteen, Professor of Chemistry
Dissertation Director

Clarence L. Grant

Clarence L. Grant, Professor of Chemistry

Colin D. Hubbard

Colin D. Hubbard, Professor of Chemistry

Gary R. Weisman

Gary R. Weisman, Associate Professor of Chemistry

Thomas M. Laue

Thomas M. Laue,
Assistant Professor of Biochemistry

Date June 28, 1988

DEDICATION

This dissertation is dedicated to Don and Maggie.

ACKNOWLEDGEMENTS

The chemistry faculty is gratefully acknowledged for their deep commitment towards education both in and out of the classroom. I would especially like to acknowledge the analytical group, Drs. Seitz, Bauer, Grant and Tomellini for giving me true appreciation for the discipline. Their ability to spark enthusiasm and to foster creative thinking directed me towards a career in academia.

Dr. Chasteen's high standards for professionalism make him a man I will always deeply admire and respect. I would like to thank him for giving me the opportunity to present my work through conferences and publications. Dr. Chasteen has demonstrated, thru example, how to properly budget and prioritize my time, for this I am deeply grateful. I thank him also for his sense of humor and especially his patience.

Members of the Chasteen group who deserve special recognition are Carmen Valdez (honorary member) and Barbara Viglione. Susan Swope, a senior member of the group is acknowledged for providing technical assistance at all times, especially during my proposal defense. Carl Thompson cheerfully passed on his knowledge of transferrin and was always there to assist during my early days. John Grady is the glue that holds the entire group together. He is a good friend and a great chemist and I wish him the

best of luck in his career. The Chasteen group would not be complete without mentioning Bill Royer. If it wasn't for Bill, I would not have made my dissertation defense deadline. Bill is credited for staying up many sleepless nights typing this entire manuscript. His support, encouragement and enthusiasm will always be remembered.

Special thanks to Marion Langan who was always there to provide comic relief and to Doris L'Abbe for her encouragement and friendship. I will always be indebted to Ray and Marlene Royer who offered me a place to live when my finances ran out. Shirley Osborne and Lilliana Richards are gratefully acknowledged for their love, laughter and prayers.

Most of all sincere thanks to Don, Maggie, Dina and Doreen ("the Phile") for giving me much needed emotional and financial support. Simply put, Dina and Doreen are the two best sisters in the world. Finally, to my parents Don and Maggie for always being there, this is your degree. For all your love and understanding you have given me throughout the years, For all the sacrifices you have made on my behalf, I dedicate this dissertation.

TABLE OF CONTENTS

DEDICATION.....	iii
ACKNOWLEDGEMENTS.....	iv
LIST OF FIGURES.....	viii
LIST OF TABLES.....	x
ABSTRACT.....	xi
	PAGE
INTRODUCTION.....	1
Transferrin.....	3
Structure.....	5
Iron Release.....	7
CHAPTER I: THE EFFECT OF MEDIATORS ON THE RATE OF IRON RELEASE FROM NATIVE AND ETHOXY- FORMYLATED DIFERRIC TRANSFERRIN.....	13
INTRODUCTION.....	14
MATERIALS AND METHODS.....	16
Transferrin.....	17
Ethoxyformylation.....	17
Iron Release Reaction.....	18
RESULTS.....	20
DISCUSSION.....	26
CHAPTER II: EFFECT OF Ru(III) MODIFICATION OF NON- LIGANDED HISTIDINES ON IRON RELEASE.....	28
INTRODUCTION.....	29
MATERIALS AND METHODS.....	32
Transferrin.....	32
Modification of Histidine.....	34
EPR Measurements.....	36
Iron-Free Modified Transferrin.....	36
Quantification of Modified Histidine Residues.....	37
Iron Release Reaction.....	40

RESULTS.....	42
Ruthenium Modification.....	42
Characterization of the Modified Complex...	43
The Iron Release Reaction.....	49
DISCUSSION.....	54
CHAPTER III: ESTIMATION OF THE DISTANCE BETWEEN THE METAL BINDING SITE AND HISTIDINE-Ru(III) COMPLEX USING ENERGY TRANSFER FLUOR- ESCENCE SPECTROSCOPY.....	57
INTRODUCTION.....	58
MATERIALS AND METHODS.....	65
Native and Modified Transferrins.....	65
Fluorescence Studies.....	66
Terbium Titrations.....	67
Overlap Integral.....	68
RESULTS.....	71
DISCUSSION.....	81
CONCLUSION.....	85
REFERENCE LIST.....	88

LIST OF FIGURES

FIGURE	PAGE
1 Schematic representation of the folding pattern and relative orientation of amino acid ligands in N-terminal lobe of transferrin.....	6
1.1 Time course of the iron release reaction for native (A) and ethoxyformic anhydride modified (B) protein using 2,3-diphosphoglycerate (DPG) as the chelating mediator.....	21
1.2 Semi-logarithmic plot of $\ln(A_{295} - A_{\infty})$ vs. time for iron removal from modified transferrin using DPG as the chelating mediator.....	22
2.1 Structure of the pentaamine ruthenium(III) histidine complex formed from reaction of histidine with aquopentaamine ruthenium(III)...	30
2.2 Working curve of flame excited emission intensity vs. ppm ruthenium for the 327.8 nm analytical line.....	44
2.3 Standard additions curves for the quantification of ruthenium in transferrin.....	45
2.4 Difference spectrum of iron-free pentaamine ruthenium(III)-histidine transferrin against apo-transferrin from 330 nm to 650 nm.....	47
2.5 $g' = 4.3$ EPR signals of diferric (A) and ruthenium modified (1.46 His residues) (B) transferrin in 100 mM HEPES, pH 7.0.....	48
2.6 Titration of Fe(NTA)_2 into iron-free, ruthenium modified transferrin. Conditions: 20 μM protein in 0.010 M HEPES, pH 7.5.....	50
2.7 Semilogarithmic plot for absorbance at 295 nm for iron release to PPI as a function of time for native (Δ) and ruthenium modified (O) transferrin in 0.1 M HEPES and 1.0 mM desferrioximine B, pH 7.16.....	51
2.8 Tsou Chen-Lu plots for kinetic data for the N-terminal site for $i = 1$, $i = 2$ and $i = 3$	53
3.1 Representation of energy transfer between a terbium ion bound to transferrin (donor) and a nearby Ru(III)-His complex (acceptor) for one of the transferrin binding sites.....	60

3.2	Energy level diagrams depicting the transitions necessary for indirect population of the 5D_4 state of transferrin-bound terbium via excitation of an adjacent aromatic group.....	62
3.3	Fluorescence emission spectra of aqueous Tb(III) and transferrin-bound Tb(III).....	72
3.4	Fluorescence emission curve for the titration of native transferrin with Tb(III).....	73
3.5	Fluorescence emission curve for the titration of ruthenium modified transferrin (5.5 His residues) with Tb(III).....	75
3.6	Fluorescence emission titration curves for native, 3.8 His residues, and 6.0 His residues modified with ruthenium(III).....	76
3.7	Tsou Chen-Lu plots of emission data for $i = 2$ and $i = 1$ (inset).....	77
3.8	Degree of spectral overlap between the Tb-trans- ferrin fluorescence emission spectrum and the pentaamine ruthenium-histidine absorption spectrum.....	79
3.9	Stereodiagram of the α -carbons in the X-ray structure of lactoferrin.....	87

LIST OF TABLES

TABLE		PAGE
I	Rate constants for iron removal from native transferrin to desferrioximine B in the presence of several chelating mediators.....	24
II	Rate constants for iron removal from ethoxyformylated diferric transferrin to desferrioximine B in the presence of several chelating mediators.....	25
III	Atomic emission instrumental parameters for the determination of ruthenium in modified transferrin.....	39
IV	IL-SLM 8000 Instrumental parameters for fluorescence using xenon arc excitation.....	69

ABSTRACT

THE ROLE OF HISTIDINE IN THE MECHANISM OF IRON RELEASE FROM HUMAN SERUM TRANSFERRIN

by

Donna M. Martin
University of New Hampshire, May, 1988

The role of non-coordinated histidines in the iron release mechanism of human serum transferrin has been investigated by chemical modification of the protein with ethoxyformic anhydride and aquopentaamine ruthenium(II), reagents specific for histidines under mild conditions. Kinetic studies of the iron release reaction at pH 5 under the action of different mediators e.g., PPI, Pi, Cit, ATP, GTP, and DPG, show that ethoxyformic anhydride imparts increased stability to the protein with rate constants for the C-terminal site decreased by factors from 2 to 10. The largest effects were seen with intracellular iron chelators GTP and DPG. A protonated imidazole group near the metal perhaps serves as a binding site for the triphosphate chelators. The binding of such chelators to a nearby histidine may assist in the formation of a quaternary intermediate of the type Chel-Fe-Transferrin-HCO₃ prior to release of iron.

Modification using aquopentaamine ruthenium(II) a reagent for surface accessible histidine residues,

enhances the rate of release from the N-terminal site but has no effect the C-terminal site. The Tsou Chen-Lu statistical method used to analyze the rate data suggests the involvement of two histidines in the N-terminal lobe not conserved in the C-terminal lobe. These results may explain the kinetic lability of the N-terminal site relative to the C-terminal site in acidic solutions.

The distance between the metal site and nearby histidines was calculated from fluorescence energy transfer measurements using Tb(III) in the iron(III) binding site as the donor and pentaamine ruthenium(III) modified histidines as the acceptor chromophore. The fluorescence measurements imply two histidines in each lobe are responsible for quenching of the Tb(III) emission. Using upper and lower limits for the index of refraction and quantum yield and assuming the energy transfer follows parallel first order kinetics, a donor-acceptor distance between 1.32 nm and 1.42 nm was obtained.

INTRODUCTION

Iron is an essential element for many metabolic processes including electron transfer reactions, deoxyribonucleotide synthesis and the transport and storage of oxygen.¹ The major form of dietary iron absorbed in the intestine is iron(II). Once in plasma, the iron(II) becomes oxidized to iron(III). Under physiological conditions however, such "free" iron(III) forms insoluble ferric hydroxides which are toxic to biological systems.² To circumvent this problem, nature has developed iron transport and storage proteins which form strong ferric complexes, thus avoiding the hydrolysis reactions inherent in the inorganic chemistry of iron(III).

Approximately 4 grams of body iron is distributed among the various iron containing proteins.³ Iron bound to hemoglobin accounts for sixty-five percent of the total. Twenty-five percent is contained in cytosolic and lysosomal ferritin, the storage protein for iron. Transferrin, the iron transport protein, accounts for less than one percent of the total iron distribution. However, all iron passes through transferrin at one time or another during its metabolism. Each molecule of transferrin cycles its iron an average of ten times in a twenty-four hour period and delivers about 100 iron atoms to iron-requiring tissues prior to the protein's catabolism by the liver.⁴

Transferrin

The transferrins comprise a class of two sited metal binding proteins distributed in blood and other bodily fluids of all vertebrates and some invertebrates.⁵ The three main types of transferrin are lactoferrin, ovotransferrin and serum transferrin.⁶⁻⁷ Ovotransferrin found in egg white and lactoferrin of milk and other secretions are bacteriostatic agents which deny invading microorganisms the iron essential for their growth.^{8,9} There is also evidence that ovotransferrin and lactoferrin play a role in protecting cells from free radical damage by sequestering catalytic iron.¹⁰ Serum transferrin, often abbreviated as transferrin, transports metabolic iron between sites of absorption, storage and utilization. Other metals which bind to the transferrins include Cu(II), Zn(II), VO(II), Mn(II), Cr(III), Tb(III) as well as other members of the transition series, actinides and lanthanides.¹¹⁻¹⁴ Whether transferrin participates to a significant extent in the transport and metabolism of these metals is unclear.

The transferrins are bilobal single chain glycoproteins having molecular weights near 80,000. They are capable of binding two iron(III) ions in separate N- and C-terminal lobes or domains. In serum transferrin, 42% of the amino acids are conserved between the two domains. The extensive homology between the lobes indicates that duplication and fusion of a structural gene

for a one-sided precursor transferrin occurred sometime during evolution.¹⁵

In order to bind iron appreciably, a synergistic anion, usually (bi)carbonate, needs to be present. This apparent cooperativity in binding is a property unique to transferrin. Another notable feature is the unusually high stability constant (10^{24} M^{-1}),¹⁶ for the iron-transferrin complex. Despite this strong binding, transferrin readily gives up its iron upon demand to cells. The understanding of this phenomenon lies in the elucidation of the mechanism of iron release and is the focus of much research in transferrin chemistry.

The proposed mechanism for iron uptake by cells involves receptor-mediated endocytosis.^{17,18} Transferrin first binds to a specific receptor on the outer cell membrane.¹⁹ The transferrin-receptor complex then becomes incorporated into an acidic intracellular compartment, the endosome. Iron is subsequently released, possibly with the aid of chelating agents (e.g. 2,3-diphosphoglycerate (DPG), adenosine triphosphate (ATP) or other phosphate compounds). Transferrin depleted of iron remains bound to the receptor and returns to the extracellular medium where it is released for another cycle of transport. The molecular mechanism of iron removal within the endosome is unknown, however.

Structure

The x-ray structure of human lactoferrin has recently been determined at 0.32 nm resolution.²⁰ The exact organization of the protein and the identity of the binding ligands is now known. The information obtained from the structure of lactoferrin can be used for serum transferrin and ovotransferrin since the complete amino acid sequences are known for all three proteins and they have many structural features in common.

The N- and C-terminal lobes are ellipsoidal with approximate dimensions 55 Å x 35 Å x 35 Å and are connected by a three turn helix. The iron sites are buried in the lobes and are approximately 42 Å apart. Each lobe can be separated further into two equal-sized domains, I and II, which describe the environment of the bound iron. Figure 1 illustrates the folding pattern and the relative orientation of the amino acid ligands. In the N-terminal lobe, residues 1-90 and 91-251 are folded in domains I and II, respectively. The chain then crosses back into domain I with residues 252-320. The same pattern is found in the C-lobe. Tyrosine-95 and Tyr-188, His-249 and Asp-63 are shown bound to the iron. The numbering of the residues corresponds to the N-terminal sequence. Previous magnetic resonance and chemical modification studies have suggested two or three tyrosines

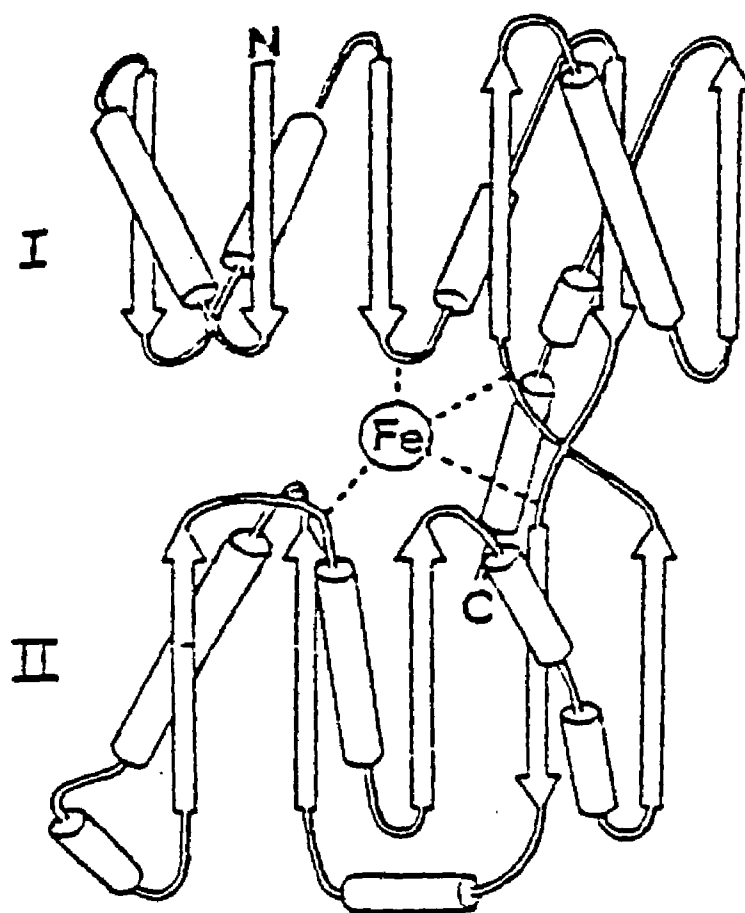


Figure 1: Schematic representation of the complex folding pattern and relative orientation of amino acid ligands in the N-terminal lobe of transferrin. Adapted from reference 20.

and one or two histidines as ligands to the metal.²¹⁻²⁴ The additional residues implicated as ligands in these studies but not found to be ligands by x-ray crystallography are presumably near the metal.

The electron density near the protein ligands suggest the presence of bicarbonate (or carbonate) and a water molecule to give an octahedral complex. The bicarbonate is positioned in the vicinity of Arg-124 in the N-terminal lobe and Arg-454 in the C-terminal lobe. These residues are thought to participate in bicarbonate binding to the protein, forming a bridge to the metal.²⁵

Iron Release

It is well established that iron release involves protonation of the iron-transferrin complex.¹ The rate of removal in the presence of chelators is first-order with respect to hydrogen ion concentration.²⁶ Thus in acidic media, the rate of iron release is greatly accelerated. As the pH of diferric transferrin is lowered, iron is first released from the N-terminal site in the pH range 7.0 - 5.5 and then from the C-terminal site between pH 5.5 and 4.0.²⁷

The reduction in thermodynamic stability of the iron-transferrin complex cannot be explained solely in terms of reduced pH, however. In the absence of chelators, transferrin can retain iron as low as pH 5.7

suggesting chelators likely play a role in iron release from the protein in-vivo.²⁸ Chelators mediate iron removal from the protein in-vitro by interacting with the bound iron, then removing and transporting it to a terminal acceptor such as desferrioximine B which has a higher affinity for iron than transferrin. Possible in-vivo chelators which may serve an intracellular transport function include ATP, DPG, guanosine 5-triphosphate (GTP) and other phosphate compounds. Bates and coworkers have proposed that the iron-transferrin-carbonate complex becomes destabilized through a transition from a "closed" to an "open" conformation, leaving the iron subject to attack by chelators.²⁹ This mechanism is consistent with recent EPR and kinetic measurements indicating the formation of a quaternary mixed-ligand Chel-Fe-Tf-CO_3^- intermediate in the iron exchange reaction where pyrophosphate is the chelator.³⁰

Examination of the x-ray structure of diferric transferrin reveals complex folding patterns which envelope the iron in each lobe (Figure 1). When iron becomes bound to transferrin, a conformational change to a more compact ordered structure occurs where amino acid ligands from three different regions of the molecule arrange to coordinate the metal. In view of the complexity of the molecule, one may envision a series of events involving mediating chelators and protein functional groups which alter the thermodynamic stability

thereby triggering a conformational change.

Experiments with diferric transferrin in the presence of the sodium salts of anions have provided evidence for the involvement of cationic functional groups in the mechanism of iron removal, possibly serving as anion binding sites for chelators. Simple salts such as NaCl and NaClO₄ alter the EPR spectrum of diferric transferrin showing that anion binding sites influence the metal centers.³¹ The presence of salts also affects the rate of iron removal from both sites. The rate of iron removal decreases at the N-terminal site and increases at the C-terminal site with increasing salt concentration.³² Different salts at the same ionic strength affect the rate of iron removal differently, showing that the effect is not solely due to changes in ionic strength. It is significant that the rate of iron release for transferrin chemically modified with acetic anhydride, a reagent specific for lysines under mild conditions, shows a similar trend, suggesting lysine as a potential anion binding site.³³

The ε-amino group of lysine, the guanidium group of arginine and the imidazole group of histidine are functional groups near the metal site which may explain the bicarbonate requirement for iron binding as well as the effects of salt and pH on the thermodynamic stability of the protein.²⁵ At physiological pH, arginine and lysine are cationic and probably contribute to iron release by

serving as binding sites for anions that can trigger conformational changes. They could also function as recognition sites, directing chelators to the iron, leading to the formation of mixed ligand complexes.

The imidazole side chain of histidine is a prime candidate for involvement in the iron release mechanism. Histidine can serve as a base by transiently accepting a proton and as an acid by transferring it again. Similarly, histidine can be both a donor and acceptor in hydrogen bonding. Clearly, interactions between non-coordinated histidine residues and the surrounding protein may well be important in the mechanism of iron removal and merit further study.

The first definitive study implicating non-coordinated histidines was done by Chasteen and Williams.³⁴ In this work the metal binding properties of transferrin were investigated using urea polyacrylamide gel electrophoresis (urea-PAGE). In the pH range 6 to 9, the relative affinity of the two sites for iron followed typical pH titration curves. The results show metal binding is influenced by the deprotonation of functional groups with pK_a values near 7.4, typical of histidine residues. EPR studies show there is no change in the first coordination sphere of the metal indicating that the groups involved are probably not coordinated to the metal.

Thompson et al.³⁵ studied the effect of chemical modification of histidine on the iron removal properties

of transferrin. Chemical modification using ethoxyformic anhydride removes the positive charge on the imidazole side chain. By spectroscopically monitoring the rate of iron removal from the modified protein by chelators, increased kinetic stability of both the N- and C- terminal sites was observed.

In the above kinetic study, the pool of reactive histidines in diferric transferrin were chemically modified to different extents. The Tsou Chen-Lu statistical method was used to analyze the rate data.³⁵ The results implied that a single modified histidine in each lobe was responsible for the observed kinetic stability of the modified protein. Examination of the amino acid sequence for conserved histidines in both lobes reveal that His-119 and His-207 in the N-terminal lobe are near the binding site and have counterparts in the C-lobe. There are also conserved histidines further away from the binding site, such as HIS-242 in the N-terminal lobe, which cannot be excluded as candidates for the key histidine, however.

The goal of this research is to further elucidate the role of histidine in the mechanism of iron release from serum transferrin. Chapters 1 and 2 concern kinetic studies of transferrin chemically modified with ethoxyformic anhydride and aquopentaammine ruthenium(II). In chapter 3, energy transfer measurements are described

to determine the distance between the metal site and modified histidine residues. If the histidine is close to the metal binding site, its role may be to direct chelators to the iron, leading to the formation of a mixed-ligand complex. If the histidine is found to be further away, then an allosteric mechanism may be involved whereby the putative histidine triggers a conformational transition which alters the iron binding properties of the protein.

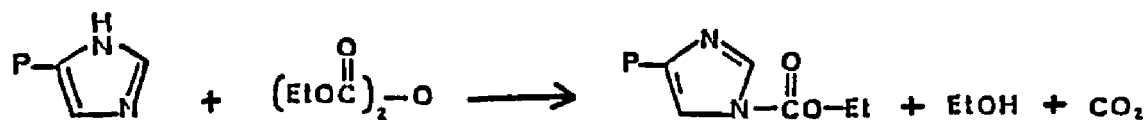
CHAPTER I

THE EFFECT OF MEDIATORS ON THE RATE OF IRON RELEASE FROM NATIVE AND ETHOXYFORMYLATED DIFERRIC TRANSFERRINS

INTRODUCTION

Much of the definitive work on the role of chelators in the release of iron from transferrin has been carried out by Morgan and coworkers.³⁶⁻³⁸ Linear dependence on $[H^+]$ in the pH range 6.0 - 7.5 was observed when chelators mediated the transfer of Fe^{3+} from transferrin to desferrioximine B.²⁶ The mediators included ATP, GTP, 2,3-diphosphoglycerate (DPG), pyrophosphate (PPi), oxalate and other compounds known to be present within cells. In another study, intracellular pH was raised by adding agents such as ammonium chloride and methylamine to the culture medium.^{39,40} The elevated pH inhibited iron release, consistent with the requirement for protonation of the iron-transferrin complex in-vivo.

Attention has been focused recently on non-coordinated amino acids of transferrin which may play a role in the iron release mechanism.^{35,41} Thompson used ethoxyformic anhydride (EFA), a reagent specific for histidine, to chemically modify diferric transferrin. The modification reaction is shown below.



The kinetics of iron removal at pH 7 were studied on diferric transferrin samples ethoxyformylated to different extents. Pyrophosphate was used as a mediator and desferrioximine B as a terminal iron acceptor. The results indicated that modification significantly decreased the rate of iron removal relative to the native protein.

In the present study the chelating mediators DPG, citrate(Cit) GTP, ATP, orthophosphate (Pi) and PPI were employed in the iron release reaction of EFA modified transferrin. These experiments were performed at pH 5 to mimic the conditions of the acidic endosome within the cell where iron release takes place. In every case, protein modification slowed the rate relative to the native protein by factors ranging from 2 to 10, thus showing that the results of Thompson were not simply due to choice of the mediator PPI.^{35,42}

MATERIALS AND METHODS

All chemicals were reagent grade and used without further purification unless otherwise stated. Glassware was washed with 6 M HCl and rinsed thoroughly with doubly distilled and deionized water (D/D H₂O) before use.

Sources of reagents were:

Human serum transferrin - Calbiochem-Behring

Sodium bicarbonate, NaHCO₃ - Baker Analyzed Reagents

HEPES (N-2-hydroxyethylpiperazine-N'-2-ethane sulfonic acid) - Research Organics stored over Chelex 100.

MES (2-(N-morpholino)-ethane sulfonic acid) - Sigma

Ferrous ammonium sulfate hexahydrate,
Fe(NH₄)₂(SO₄)₂·6H₂O - Baker Analyzed Reagents

EFA (ethoxyformic anhydride), C₆H₁₀O₅ - Aldrich

Sodium perchlorate, NaClO₄ - Baker Analyzed Reagents

Desferrioximine B, C₂₆H₅₂N₆O₁₁S - Ciba

Sodium pyrophosphate decahydrate, Na₄P₂O₇·10H₂O
-Aldrich

Sodium citrate pentahydrate, Na₃C₆H₅O₇·5H₂O
-Mallinckrodt

Sodium phosphate dodecahydrate, Na₂HPO₄·12H₂O - Sigma

ATP (adenosine triphosphate) - Aldrich

GTP (guanosine 5'-triphosphate) - Sigma

DPG (2,3-diphosphoglycerate) - Sigma

Transferrin

Iron-free, lyophilized human serum transferrin (500 mg) of stated 98-99% purity was dissolved in 5 mL of D/D H₂O. To eliminate reducing agents non-specifically bound to the protein of commercial preparations, the protein solution was then dialyzed against three changes of 0.10 M sodium perchlorate pH 7.0 - 8.0, followed by three changes of 0.010 M HEPES and 0.010 M NaHCO₃ at pH 7.5 - 8.0 (2 L per change). The concentration of apotransferrin was determined spectrophotometrically with a Cary 219A or Bausch and Lomb 505 spectrophotometer using a molar absorptivity, $\epsilon_{280\text{nm}} = 8.89 \times 10^4 \text{ M}^{-1}\text{cm}^{-1}$.⁴³

Diferric transferrin in 0.10 M HEPES and 0.020 M NaHCO₃ was prepared by adding 0.01 M ferrous ammonium sulfate in 0.01M HCl to the transferrin solution to 97% iron saturate the protein. The solution was left to equilibrate for 10 - 12 hours to ensure maximum binding of the iron. The final degree of saturation achieved was determined by measuring the absorbance at 465 nm using $\epsilon_{465\text{nm}} = 5000 \text{ M}^{-1}\text{cm}^{-1}$ per molecule of diferric protein.⁷ Typical levels of saturation obtained were 77 - 91%.

Ethoxyformylation

Ethoxyformic anhydride (EFA) was gradually added in microliter amounts to a stirred solution of 3.8 - 4.0 μM diferric transferrin in 0.10 M HEPES, 0.10 M NaHCO₃ at pH 7.4, to a final concentration of 1.0 - 2.0 mM EFA. The

modification reaction was monitored by uv difference spectroscopy at 242 nm with native diferric transferrin in the reference cell. The extent of modification was calculated using a molar absorptivity $\epsilon_{242\text{nm}} = 3200 \text{ M}^{-1}\text{cm}^{-1}$ per histidine monoethoxy-formylated.⁴⁴ Low molecular weight products were removed by ultrafiltration using an Amicon cell fitted with a PM10 membrane having a molecular weight exclusion limit of 10,000. The volume was replaced three times (90% V/V per change) with fresh 0.01 M HEPES at pH 7.0 - 7.4.

Iron Release Reaction

The rate of iron removal from native and ethoxyformylated diferric transferrin was monitored at 295 nm using a Cary 219A spectrophotometer interfaced with an Apple IIe computer. The sample cells were thermostatted to $25.0^{\circ}\text{C} \pm 0.1^{\circ}\text{C}$. The cells were optically balanced at 295 nm using D/D H_2O . The D/D H_2O in the sample cell was then replaced with 1.2 mL of 12 - 20 μM protein in dilute 5 mM HEPES at pH 7.0. A reaction solution (68 μL) of 0.10 M mediator (sodium salts of Cit, PPI, Pi, ATP and DPG), 0.02 M desferrioximine B in 1.0 M MES at pH 5.0 was added to the the sample and reference cuvettes to obtain a final concentration of 3 mM in mediator. When GTP was used as the mediator, a reaction solution (68 μL) of 2.0 mM GTP, 0.20 M desferrioximine in 1.0 M MES was used and added to both cells (1.0 mL) giving a final concentration of $1.20 \times$

10^{-4} M GTP. The decrease in absorbance as a function of time was typically recorded using Apple IIe kinetic software.

The pseudo first-order macroscopic rate constant for iron removal from the C-terminal binding site, k_C , was determined by linear regression using Equation 1.

$$\ln(A_{295} - A_{\infty}) = \ln(A_0 - A_{\infty}) - k_C t \quad (\text{Eq. 1})$$

RESULTS

Kinetic studies were carried out on completely modified transferrin in order to deactivate the histidine residues involved in the iron release reaction. Concentrations of ethoxyformic anhydride ranging from 1.3 - 1.5 mM resulted in the modification of 14.0 - 15.1 histidine residues on diferric transferrin at a concentration of 4 μ M. The values obtained here for extensively modified transferrin are consistent with those previously reported.^{24,41} (Out of 18 total residues, ~4 histidines on diferric transferrin are unreactive toward EFA.)³⁵

Ethoxyformylation had the greatest effect on the rate of iron removal when 2,3-diphosphoglycerate (DPG) was employed as the mediating chelator. The increased kinetic stability is shown in absorbance vs. time curves for native and modified transferrin using DPG (Figure 1). The times for removal of 90% of the iron from the protein are 3.0 min and 23 min for native and modified transferrin, respectively. The macroscopic rate constant for the C-terminal site was extracted from semilogarithmic plots (Figure 1.2). All six mediators showed similar biphasic kinetics, however, iron removal from the N-terminal site was too fast to obtain a reliable macroscopic rate constant for this site using conventional spectrophotometry.

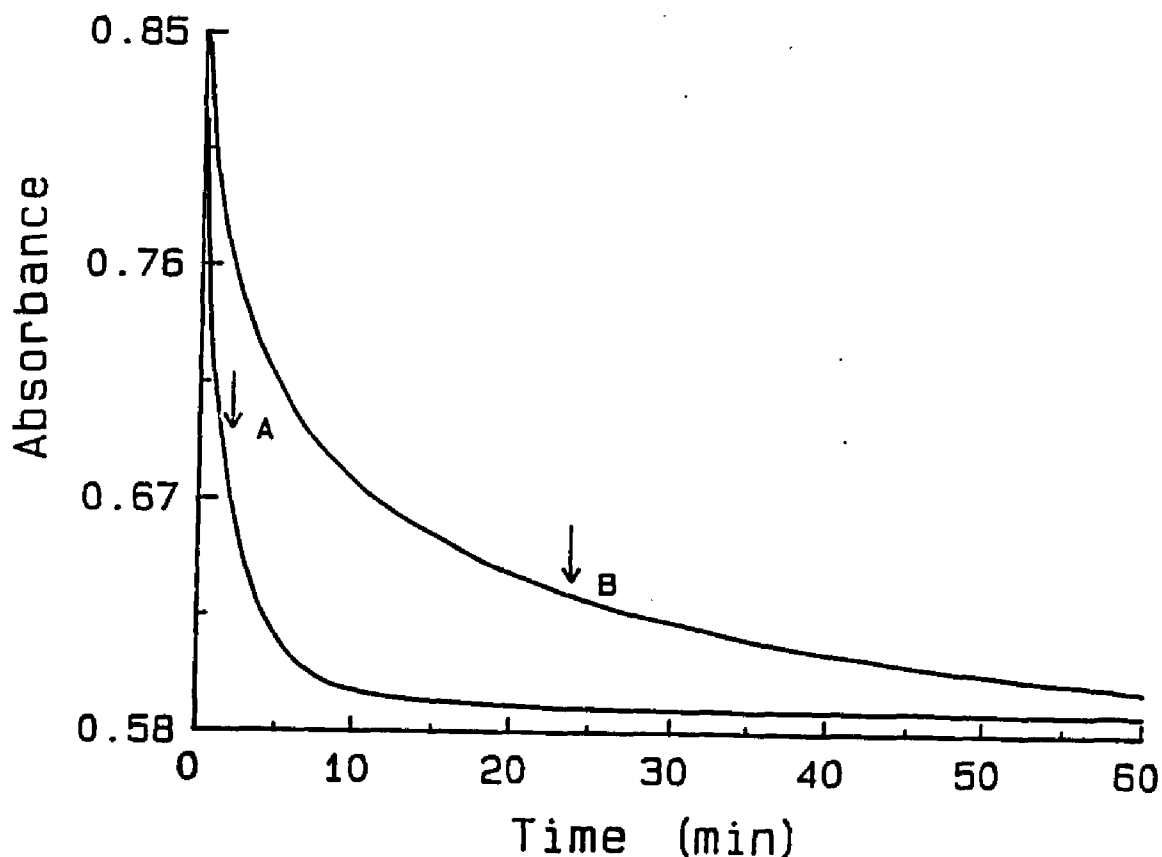


Figure 1.1: Time course of the iron release reaction at 295 nm for native (A) and modified (B) protein using 2,3-diphosphoglycerate (DPG) as chelating mediator. Conditions: (A) 16.0 μM native diferric transferrin, 3 mM DPG, 1.3 mM desferrioximine B, 0.064 M MES, pH 5.20, 25 C. (B) 18.0 μM modified transferrin (14 histidine residues ethoxyformylated), pH 5.19, same conditions as curve (A). The arrows indicate the times for 90% iron removal. FILES: DPGNAT, DPGMOD, Disk #1.

The macroscopic rate constants for the C-terminal site for 90% iron removal from native and modified transferrins by various mediating chelators are listed in Tables I and II. Overall, the rates are markedly faster at pH 5 when compared with previous studies at pH 6.9 conducted under otherwise similar conditions of 5 mM mediator and 5 mM desferrioxime B.^{35,38}

The relative rate of iron removal in native transferrin at pH 5 under the action of 6 different mediators follows the order GTP > DPG > PPI > ATP > citrate > Pi. In contrast, the relative rates for modified transferrin in Table II follow the order PPI > GTP > ATP > citrate ~ phosphate > DPG. Ethoxyformylation imparted the greatest rate differences when DPG and GTP are used as mediators. Modification affected iron removal mediated by orthophosphate the least.

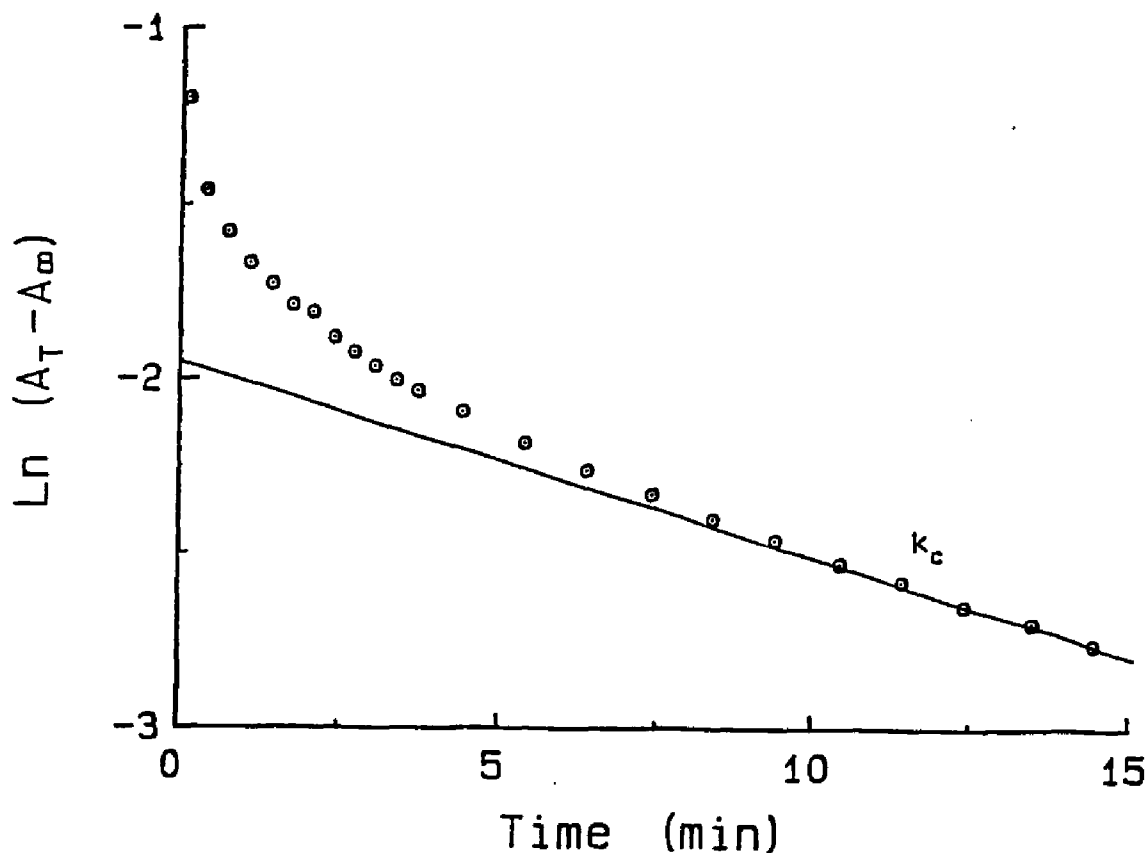


Figure 1.2: Semilogarithmic plot of $\ln (A_{295} - A_\infty)$ vs. time for the iron removal of modified transferrin using 2,3-diphosphoglycerate (DPG) as mediating chelator. Conditions: 18.0 μM modified diferric transferrin (14.0 His modified), 3.0 mM DPG, 1.3 mM desferrioximine B, 0.064 M MES, pH 5.19, 25 C. The macroscopic rate constant for the C-terminal site, k_c , was measured by linear regression on the linear portion of the second phase of the above plot employing the last 8 points. The N-terminal site was too fast to obtain a rate constant using conventional spectrophotometry. FILE: SLDPGM Disk #1.

Table I
NATIVE PROTEIN^a

Mediator	Rate Constant (min ⁻¹) ^b	Time for 90% Fe Removal (min)	pH ^c
citrate	0.18 ± 0.01	5.3	5.11
	0.18 ± 0.01	5.6	5.14
phosphate	0.14 ± 0.01	8.0	5.05
	0.16 ± 0.02	12.6	5.12
	0.16 ± 0.01	12.6	5.14
pyrophosphate	0.55 ± 0.05	2.1	5.12
	0.55 ± 0.03	2.2	5.14
ATP	0.34 ± 0.04	2.5	5.00
DPG	0.69 ± 0.03	3.0	5.20
GTP ^d	0.90 ± 0.08	1.0	4.77

^aConditions: 12.0 - 20.0 μM native diferric transferrin
1.3 mM desferrioximine B, 0.064 M MES, 3 mM mediator
25.0 ± 0.1°C.

^bReplicate determinations shown. Confidence intervals
for the standard deviation of the slope given at the 95%
probability level.

^cMeasured at completion of the reaction.

^dThe concentration of GTP was diluted 50-fold relative
to the other mediators due to its high absorbance
at 295 nm. Fifty-fold dilution for di- and tri-
phosphate mediators decrease the rate of iron removal
by factors ranging from 2 to 4.²⁶ The rate constant has
been corrected by assuming a 50-fold dilution will
decrease the iron removal rate at least 2-fold.

Table II
MODIFIED PROTEIN^a

Mediator	Rate Constant (min ⁻¹) ^b	Time for 90% Fe Removal (min)	pH ^c
citrate	0.11 ± 0.01	12.0	5.03
	0.093 ± 0.01	12.0	5.12
phosphate	0.11 ± 0.01	26.0	4.80
pyrophosphate	0.23 ± 0.02	9.5	4.99
	0.24 ± 0.04	9.5	4.99
ATP	0.11 ± 0.01	13.0	4.98
	0.16 ± 0.03	11.4	4.98
DPG	0.055 ± 0.002	23.0	5.19
GTP ^d	0.20 ± 0.02	12.7	4.67

^aConditions: 12.0 - 20.0 μM modified diferric transferrin (14.0 - 15.1 His residues ethoxyformylated), 1.3 mM desferrioximine B, 0.064 M MES, 3 mM mediator 25.0 ± 0.1°C.

^bReplicate determinations shown. Confidence intervals for the standard deviation of the slope given at the 95% probability level.

^cMeasured at completion of the reaction.

^dThe concentration of GTP was diluted 50-fold relative to the other mediators due to its high absorbance at 295 nm. Fifty-fold dilution for di- and tri-phosphate mediators decrease the rate of iron removal by factors ranging from 2 to 4.²⁶ The rate constant has been corrected by assuming a 50-fold dilution will decrease the iron release rate by a least 2-fold.

DISCUSSION

The kinetic experiments described demonstrate that the decrease in the rate of iron release when the protein is modified is not unique to the mediator pyrophosphate employed in previous studies.^{35,42} Indeed the effect is seen with a variety of mediators (Tables I & II) and supports the hypothesis that histidine residue(s) play a role in the mechanism of iron removal from transferrin.

The relative order of the rates of iron release with different mediators is in accord with the work of others. The kinetic studies of Carver and Friedman at pH 6.1 gave the following order for both sites: PPI > GTP ~ ATP ~ DPG > Cit > Pi.⁴⁵ The rate of chelator-mediated iron exchange at neutral pH between rabbit and human transferrin followed the order GTP > DPG > ATP > Cit > PPI > Pi. Except for PPI, the order parallels the rates observed in the present study at pH 5. The high affinity of PPI for iron, relative to the other mediators, perhaps explains the low rate of iron exchange with pyrophosphate.³⁶

The most effective mediators were DPG, ATP and GTP which are present in mM concentrations in iron requiring cells.^{45,46} Of particular interest is the marked effect that ethoxyformylation of histidine has upon DPG and GTP in releasing iron from transferrin. The results are consistent with the idea that a protonated imidazole group

near the metal serves as a binding site for the larger di- and triphosphate mediators. This would account for the more pronounced effect of modification on iron release when DPG, ATP and GTP are used as mediators. The neutralization of positive charge on the imidazole group resulting from EFA modification would inhibit the binding of these anionic chelators to histidine. Binding of chelators to the imidazole group of histidine possibly assists in the formation of a Chel-Fe-transferrin- CO_3 intermediate complex which subsequently releases iron as a Chel-Fe complex where Chel is GTP, ATP or DPG. The presence of ATP and GTP iron complexes in red blood cells lends support to this mechanism.^{47,48} These complexes are stable at physiological pH and have strong formation constants in acidic media (e.g. $K_{\text{Fe-ATP}} \sim 4 \times 10^6$ at pH 2).⁴⁹ Their stability in acid makes them capable of forming in the acidic endosome and provide a means for intracellular iron transport at physiological pH as well.

While a histidine effect has been reasonably well established from in-vitro experiments in this laboratory, direct evidence for the involvement of non-coordinated histidine in the cellular uptake of iron within the cell has not been established and certainly merits further study.

CHAPTER II

EFFECT OF Ru(III) MODIFICATION OF NON-LIGANDED HISTIDINES ON IRON RELEASE

INTRODUCTION

The chemistry of ruthenium(II) and ruthenium(III) amine complexes has been an area of considerable activity in recent years. Several ruthenium compounds have been shown to interfere with DNA synthesis and exhibit anti-tumor activity in animals.^{50,51} Pentaammine ruthenium(III) complexes have been used to investigate conformational changes in proteins.⁵² Electron transfer reactions of metalloproteins using pentaammine ruthenium bound to histidine as a redox-active metal complex have also been carried out.⁵³⁻⁵⁸

Reactions involving aquopentaammine ruthenium and model compounds, in neutral and acidic aqueous solutions give octahedral pentaammine-histidine complexes where bonding is through the N-3 nitrogen of the imidazole ring (Figure 2.1).⁵⁹ Titration with sodium hydroxide results in intense charge transfer bands at pH 10. In aqueous solutions which are not strongly acidic, pentaammine ruthenium complexes of π -acceptor ligands like histidine are relatively unreactive and undergo substitution very slowly or not at all.⁶⁰ The slow ligand exchange rate is consistent with the observed stability of the complex.

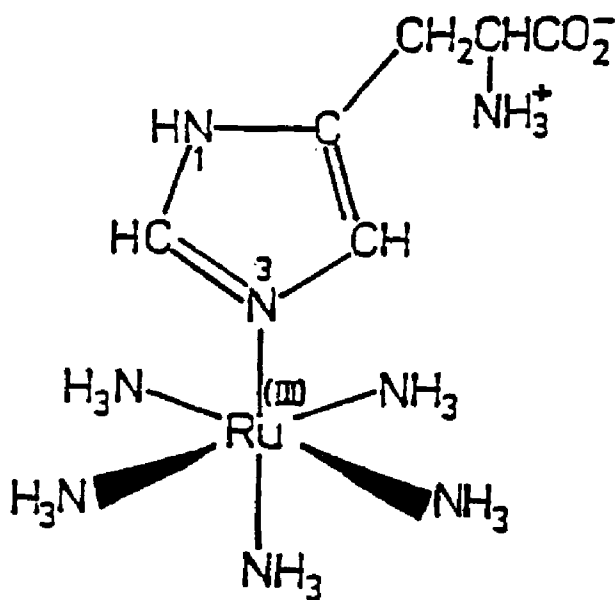


Figure 2.1: Structure of pentaammine ruthenium(III)-histidine complex formed from reaction between histidine and aquopentaammine ruthenium(II). Optical and NMR studies indicate bonding through the N-3 "pyridine nitrogen" of the imidazole ring resulting in charge transfer bands at 365 and 600 nm at pH 10⁵⁹. Figure adapted from reference 66.

Several chemical modification studies involving aquopentaammine ruthenium(II) and proteins demonstrate that the reagent has a strong preference for surface accessible histidine residues.^{61,65} Other nucleophilic groups such as lysines and methionines are potential candidates for modification. However, under the mild conditions employed in these studies, aquopentaammine ruthenium(II) reacts only with imidazole moieties.⁶¹⁻⁶⁵ Matthews and coworkers have modified histidines in ribonuclease A⁶¹, α -Lytic protease⁶², and lysozyme.⁶² Gray et al. studied the effects of histidines modified with aquopentaammine ruthenium(II) in horse heart ferricytochrome c⁶³, pseudomonas aeruginosa azurin⁶⁴, and sperm whale myoglobin.⁶⁵

In this chapter studies of the ruthenium modification of histidines on diferric and C-terminal transferrins are described. The results show that modification kinetically destabilizes the N-terminal site whereas modification does not significantly affect the C-terminal site. The data implies two non-coordinated histidines in the N-terminal domain are responsible for the observed kinetic effects.

MATERIALS AND METHODS

All glassware was soaked in 6 M HCl and thoroughly rinsed with doubly distilled, deionized water. Sodium perchlorate and HEPES were treated with Chelex 100 before use. Chelex 100 (Sigma, sodium form dry mesh 50-100) was made to the hydrogen form by passing copious amounts of 1.0 M HCl through a fritted glass funnel, followed by rinsing with 0.10 M prechelexed NaOH. The pH of the effluent was adjusted to 6 by washing with D/D H₂O. All chemicals were reagent grade, unless otherwise stated, and obtained from the following sources.

TRIS-HCl(Tris[hydroxymethyl]aminomethane hydrochloride)
-Sigma

Sodium perchlorate - Aldrich

Nitrilotriacetate (disodium salt) - Sigma

Chloropentaammine ruthenium dichloride - Alfa

Cesium chloride (ultra-pure) - Sigma

Iron AA standard - Fisher Scientific

Ruthenium AA standard - Aldrich

Zinc metal granular 20 mesh - Mallinckrodt

Mercury metal (triply distilled)

Argon (research grade 4.8) - Airco

Transferrin

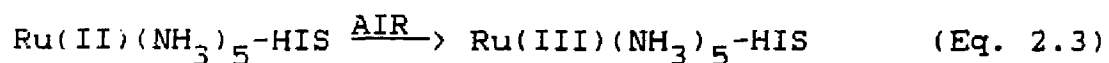
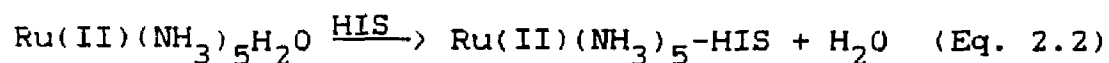
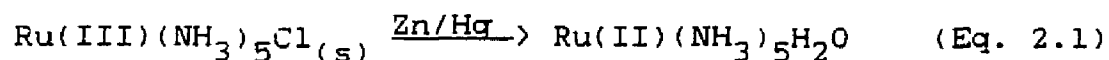
Iron-free human serum transferrin was prepared and assayed as described in Chapter I. Diferric transferrin (0.2 - 0.4 mM) was prepared by addition of 5.00 mM iron(III):nitrilotriacetate (1:2) Fe(NTA)_2 , pH 4.0, calculated to 100% saturate the protein. Excess NTA was removed by dialysis against three changes of 0.10 M NaClO_4 , 0.01 M HEPES, pH 7.0 - 8.0, followed by three changes of 0.020 M HEPES pH 7.0 - 7.4. The percent saturation (85 - 93%) was determined spectrophotometrically using the molar absorbtivity $\epsilon_{465\text{nm}} = 2500 \text{ M}^{-1}\text{cm}^{-1}$ per bound iron.⁴¹ The percent destribution between the N- and C-terminal sites was determined by urea-polyacrylamide gel electrophoresis (UREA-PAGE) using the method of Chasteen and Williams.³⁴

C-terminal monoferric transferrin was prepared by performing a preliminary difference titration using a CARY 219A spectrophotometer. The cells were balanced with 0.1 mM apotransferrin in 0.10 M HEPES and 20 mM NaHCO_3 , pH 7.3 - 7.4. Microliter aliquots of Fe(NTA)_2 were added to the sample cuvette and the absorbance scanned between 460 - 470 nm. After determination of the titration endpoint, Fe(NTA)_2 was added to a 0.2 mM stock apotransferrin solution in 0.10 M HEPES, 0.020 M NaHCO_3 pH 7.3 - 7.4 to 47% saturate the protein. Excess NTA was removed by dialysis against 0.10 M NaClO_4 in 0.010 M HEPES, pH 7.3 -

7.4, followed by dialysis against 0.025 M HEPES pH 7.3 - 7.4. The purity of the C-terminal preparation was determined using urea-PAGE as previously described. The stock monoferric solution was then frozen until further use.

Modification of Histidine

The modification of histidines on diferric transferrin using the aquopentaammine ruthenium(II) reagent proceeds in three steps.



The aquopentaammine ruthenium(II) reagent was generated by reduction of chloropentaammine ruthenium(III) dichloride using a Zn/Hg amalgam. The reduction and subsequent modification was performed under a continuous purge of argon to prevent the aquopentaammine

ruthenium(II) complex from reacting with molecular nitrogen.

The amalgam was prepared by grinding 7.2 grams of Zn flakes with 78 grams of Hg in 10 mL of 0.5 M H_2SO_4 with a mortar and pestle.⁶⁷ The acid was decanted and the amalgam washed three times with D/D H_2O and once with 0.250 M HEPES, pH 6.8 - 6.9, and then transferred to a 250 mL round bottom flask. Chloropentaammine ruthenium(III) dichloride (50 - 200 mg) in 20 - 125 mL of 0.250 M HEPES, pH 6.8 - 6.9 was added to the amalgam. Chloropentaammine Ru(III) is insoluble in aqueous solution and dissolves only upon reduction. The reaction is complete when a clear bright yellow solution is obtained. Reaction time is typically 2 - 3 days.

The aquopentaammine Ru(II) complex is decanted into a 250 mL three-neck flask equipped with a spin bar. Twenty-four mL of 100 μM diferric or C-terminal transferrin in 0.250 M HEPES pH 6.8 - 6.9 is divided into 4 mL aliquots and placed into dialysis bags. The reduced ruthenium complex readily diffuses through and reacts with the protein. The protein in the dialysis bag is removed from the ruthenium solution after various times (3 hours to 4 days) and the Ru(II) oxidized by placing the dialysis bag in 1 L of a 0.250 M TRIS solution, pH 7.0, with aeration for 12 hours. This procedure oxidizes the ruthenium(II)-HIS complex to the stable trivalent state and removes the unreacted ruthenium reagent. Following air

oxidation, the protein (~4 mL) is centrifuged and subsequently dialyzed against two changes (2 L each) of 0.010 - 0.020 M TRIS pH 7.0 and once against 2 L of 0.010 - 0.020 M HEPES pH 6.8 - 7.0.

EPR Measurements

EPR measurements were made on solutions frozen at 77 K with a Varian E-4 spectrometer equipped with a liquid N₂ dewar inset. Instrumental settings were:

Field Set	= 1500 G
Scan Range	= 2000 G
Modulation Amplitude	= 8.2 G
Time Constant	= 1.0 s
Microwave Power	= 10 mW
Scan Time	= 8 min
No. of Data Points	= 2000

Double integral values were calculated from spectra to which a linear baseline correction had been applied.

Iron-Free Modified Transferrin

Iron-free modified transferrin was prepared from 50 µM protein upon addition of pyrophosphate, desferrioximine B and MES buffer with final concentrations 50 mM, 3 mM and 0.10 M respectively. The pH of the solution was adjusted

to 5.0 with 0.1 - 0.5 M HCl and allowed to equilibrate for 10 - 12 hours. In order to quantitatively remove iron, the protein was exhaustively dialyzed using five changes of 0.010 M TRIS pH 6.8 - 7.0 (2 L each) followed by 2 L of 0.010 M HEPES pH 6.8 - 7.0. The extent of iron removal from the protein was determined by EPR measurement of the $g' = 4.3$ signal. The modified apoprotein was assayed spectrophotometrically at 280 nm using a molar absorptivity of $\epsilon_{280\text{nm}} = 8.89 \times 10^4 \text{ M}^{-1}\text{cm}^{-1}$.⁴³

Quantification of Modified Histidine Residues

The concentration of Ru in $\text{Ru(III)(NH}_3)_5\text{-HIS}$ transferrin was determined by measurement of the 372.8 nm Ru emission line using a nitrous oxide-acetylene flame. An Instrumentation Laboratories IL 951 dual channel AA/AE spectrometer was used for the analysis following an established protocol.⁶⁸ Optimum signal was obtained using instrumental parameters described in Table III. Channel B measured emission intensity at 372.8 nm. Channel A was set 1.3 nm from the analytical line and was used to monitor background emission.

Cesium chloride (1000 ppm) was added to all samples and standards in order to suppress ruthenium ionization. Optimization of emission intensity was done using a 20 ppm RuCl_3 standard and a blank containing 1000 ppm CsCl and D/D H_2O . The parameters varied were wavelength, burner height and fuel-oxidant ratio. It is critical to operate

with very lean fuel, otherwise complete quenching of the signal occurs due to intense background emission from cyanogen at 365 - 390 nm, characteristic of a fuel-rich flame. During optimization and analysis the burner head was periodically scraped to avoid clogging.

A calibration curve was established for each run using a series of seven standard RuCl_3 solutions in the 1 - 50 ppm range. The standard addition method was used to compensate for chemical interference arising from the protein matrix. A three or four point standard curve was generated for each protein analyzed, the amount of added Ru ranging from 0 - 3 ppm. Typically, 2 - 10 μM of modified apoprotein (1.25 mL) was aspirated into the flame. The concentration of protein employed was chosen to minimize sample consumption for the extent of ruthenium modification of each sample.

Samples, standards and blanks (one blank per four samples) were run in random order. Readings were taken in triplicate with each reading averaged over 2 - 3 seconds. The mean standard deviation and relative standard deviation were calculated by the IL 951 microcomputer. Linear regression for the generated standard addition curve was performed on each sample. The histidines modified per mole of transferrin was then calculated.

Table III

Atomic Emission Instrumental Parameters^a

Burner Head : N₂O single-slot standard burner head
Flame Description : N₂O-acetylene, fuel lean with 5 mm red
feather
Fuel/Oxidant : 0.70
Aspiration Rate : 5.2 - 5.4 mL/min
Burner Height : variable
Scale Expansion : 1.0

	<u>Channel A</u>	<u>Channel B</u>
Wavelength :	374.1 nm	372.8 nm
Bandpass :	1.0 nm	0.3 nm
Photomultiplier		-
Voltage :	900 - 1000	900 - 1000

^a IL 951 Instrumentation Laboratories AA/AE Spectrometer

Alternate emission wavelengths for Ru are 379.9 nm, 349.9 nm
and 342.8 nm.⁶⁸

The formation of $\text{Ru(III)(NH}_3)_5\text{-His}$ complex was determined by uv/vis difference spectroscopy. Apo-transferrin (6 μM) at pH 10.0 was balanced in both the sample and reference cells. Modified apoprotein (pH 10.0) at the same concentration was then substituted in the sample cell and the absorbance scanned from 500 nm to 325 nm. The molar absorptivity used for calculation was $\epsilon_{365\text{nm}} = 3350 \text{ M}^{-1}\text{cm}^{-1}$ per Ru-His formed.⁵⁹

Iron Release Reaction

The rate of iron removal from native and Ru modified transferrin was monitored at 295 nm using a CARY 219A spectrometer thermostatted to $25.0^\circ\text{C} \pm 0.1^\circ\text{C}$. The cells were initially balanced at 295 nm using 0.10 M HEPES, pH 7.0. The sample cell was then replaced with 10 - 15 μM protein in 0.10 M HEPES at the same pH. A reaction solution of 0.10 M pyrophosphate and 0.020 M desferrioximine B was added to the sample and reference cells to obtain a final concentration of 3 mM in pyrophosphate. Absorbance vs. time curves for diferric proteins were fitted to Equation 2.4 using RS-1 software on the VAX 11/780 computer.

$$A_{295} = (A_0 - A_\infty)(X_N \exp(-k_N t) + X_C \exp(-k_C t)) + A_\infty \quad (\text{Eq 2.4})$$

where k_N and k_C are the pseudo-first order macroscopic rate constants for iron removal from the N- and C-terminal sites. X_N and X_C are the mole fractions of iron in the two sites. For C-terminal transferrin, a linear regression was used to determine the macroscopic rate constant using Equation 1.1 in chapter I.

A Tsou Chen-Lu plot was used to analyze the kinetic data for the N-terminal site. The Tsou Chen-Lu method is a graphical technique used to determine the number of essential residues responsible for a change in activity in a chemically modified protein.⁶⁹ The activity, a , can be any experimental quantity. The relationship is given by $a^{1/i} = X$, where a is the activity and X is the mole fraction of unmodified residues in a pool of equally reactive residues. A linear plot of $a^{1/i}$ vs. X is obtained upon proper choice of i ($i = 1, 2, 3, \dots$), the number of essential residues.

RESULTS

Ruthenium Modification

In addition to the procedure described in the methods section, preliminary experiments included reducing the Ru(III) salt electrochemically using Pt electrodes held at a constant potential of 1.2 volts. This reduction procedure led to undesirable side reactions observed by the absence of yellow color due to the $\text{Ru(II)(NH}_3)_5\text{H}_2\text{O}$ species and by the presence of brown precipitate at reaction times greater than 6 hours. This procedure therefore was not studied further.

Reduction of $\text{Ru(III)(NH}_3)_5\text{Cl}$ using a Zn/Hg amalgam proceeded successfully, producing a bright yellow solution in 2 - 3 days. After solubilization of the Ru(III), salt the reaction went through an intermediate peach color presumably due to the formation of $[\text{Ru}^{\text{II/III}}(\text{NH}_3)_5\text{Cl}]_2$.⁶⁰ The conditions employed here (Materials and Methods) modified 6.0 histidine residues per mole of diferric protein and 8.1 histidines per mole of C-terminal monoferric transferrin for 48 - 60 hr reaction times. Protein exposed to longer reaction times produced considerable precipitate. Analysis by EPR and spectrophotometry indicated that a significant amount of Fe did not remain bound to the protein at reaction times greater than 60 hours. Long reaction times also led to

the appearance of an unknown band occurring at 270 - 300 nm. The band could be due to modification of methionines;⁶⁹ however, this assignment has not been verified. Due to the difficulties encountered with long reaction times, diferric and C-terminal monoferric transferrin are said to be extensively modified at values of 6.0 and 8.1 per mole. of protein, respectively, corresponding to reaction times of ~50 hr.

The number of residues modified per mole of transferrin was determined using atomic emission spectrometry with background correction (Materials and Methods). A typical working curve for Ru at 372.8 nm is shown in Figure 2.2 for a fuel-lean nitrous oxide - acetylene flame. The linear range varied from 0 - 5.8 ppm to 0 - 10 ppm between runs, however. Quantification by the working curve method gave positive deviations due to the physical and chemical interferences arising from the protein matrix. Therefore, the standard additions method was chosen to measure Ru in the protein (Figure 2.3).

Characterization of the Modified Complex

The formation of the pentaammine ruthenium-histidine complex in diferric transferrin was determined by comparing the optical spectra of modified apotransferrin with that of pentaammine ruthenium-histidine trichloride, a model for the transferrin complex.⁵⁹ The difference spectrum of iron-free Ru modified (6.0 His residues) vs.

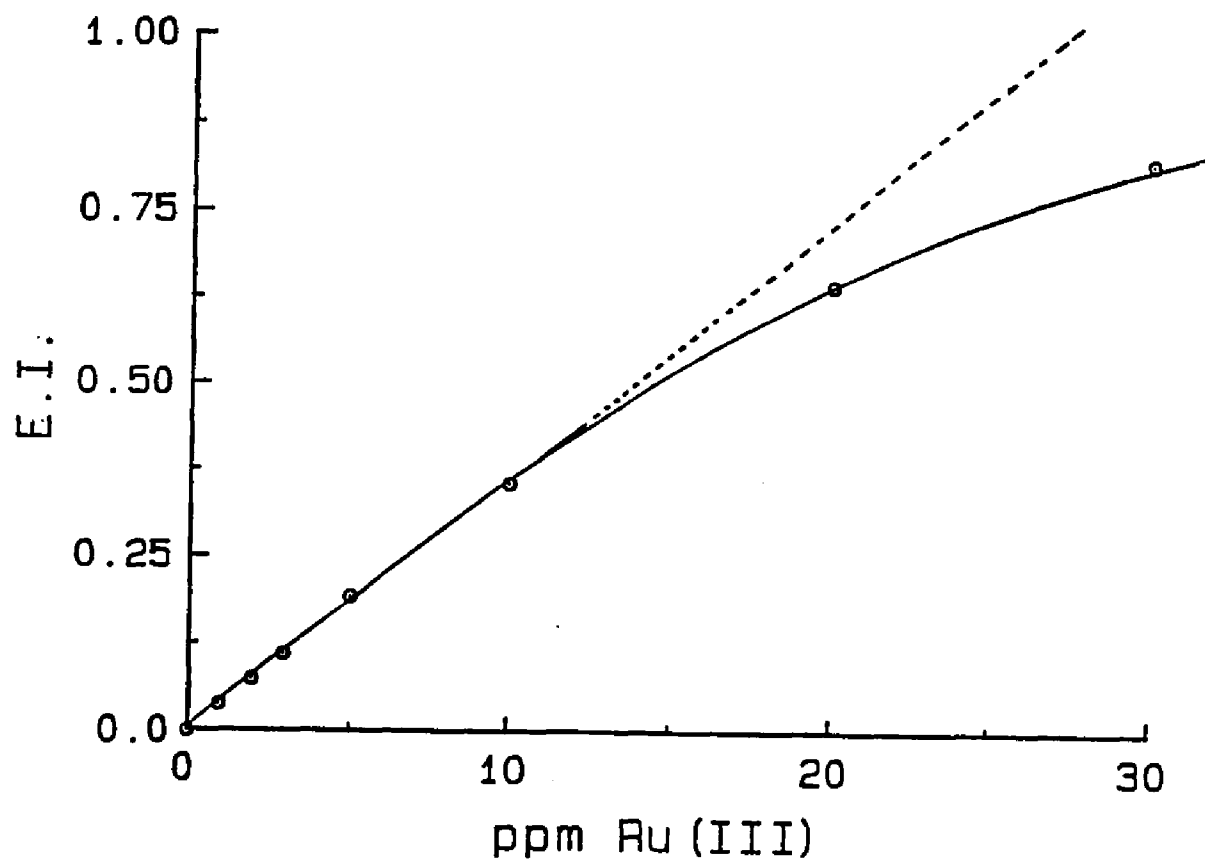


Figure 2.2: Calibration curve of emission intensity vs. ppm ruthenium for the 327.8 nm analytical line (see Materials and Methods). The linear portion of this curve is from 0 to 10 ppm. This linear range varied between runs. Quantification of bound ruthenium in the protein matrix gave positive deviations with the working curve method. FILE: RUWCI Disk #3.

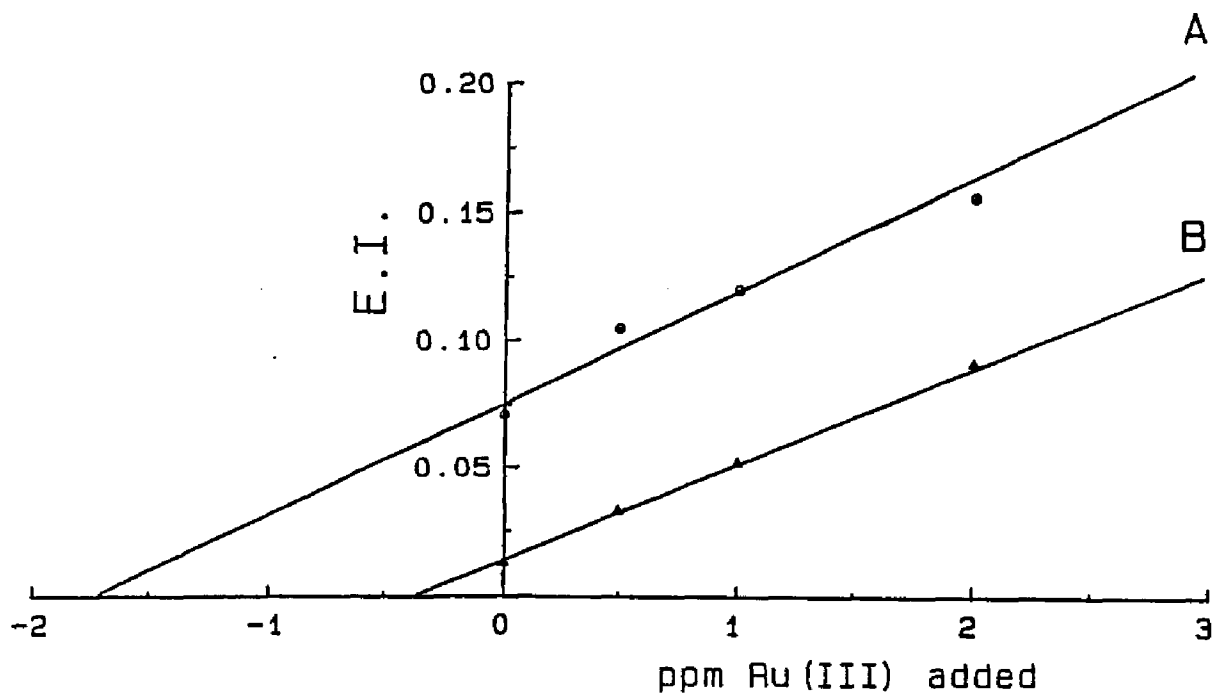


Figure 2.3: Standard additions plots for the quantification of ruthenium in transferrin. Linear portion of the working curve used (see Materials and Methods). Shown are typical standard addition curves which were generated for each transferrin sample analyzed. Linear regression shows 1.72 ppm (3.4 modified residues) for A and 0.339 ppm (0.425 modified residues) for B.

native protein at pH 10 is shown in Figure 2.4. An intense band occurs at 377 nm and a broader, less intense band is found from 510 - 620 nm. Bands of similar intensity and width are found for the model compound at 365 and 600 nm at pH 10.¹⁰ The bands are due to ligand-to-metal charge transfer transitions between the deprotonated imidazole and the ruthenium. The bands for protonated imidazole on the model compound are less intense and occur at 303 nm and 450 nm at pH 5. A pK_a of 8.87 for the N_1 nitrogen on imidazole has been reported.⁵⁹ The pH behavior observed for modified transferrin is consistent with the spectral shift of the model compound.

No change in the optical spectrum occurred upon ultrafiltration (3 changes of fresh 0.01 M HEPES, pH 7, 90% V/V each change) or upon storage at pH 7 at 4°C for 6 weeks. Long term stability of the modified protein is in accord with ruthenium amine complexes stored in aqueous solution at neutral pH (ruthenium complexes of π acceptor ligands such as imidazole are labile and can undergo ligand substitution under acidic conditions, however).

Little difference is observed in the characteristic $g' = 4.3$ EPR signal between native and modified diferric transferrins, indicating that no gross changes in the Fe binding sites occur upon modification (Figure 2.5). Comparison of linewidths show no paramagnetic line broadening due to ruthenium incorporation.

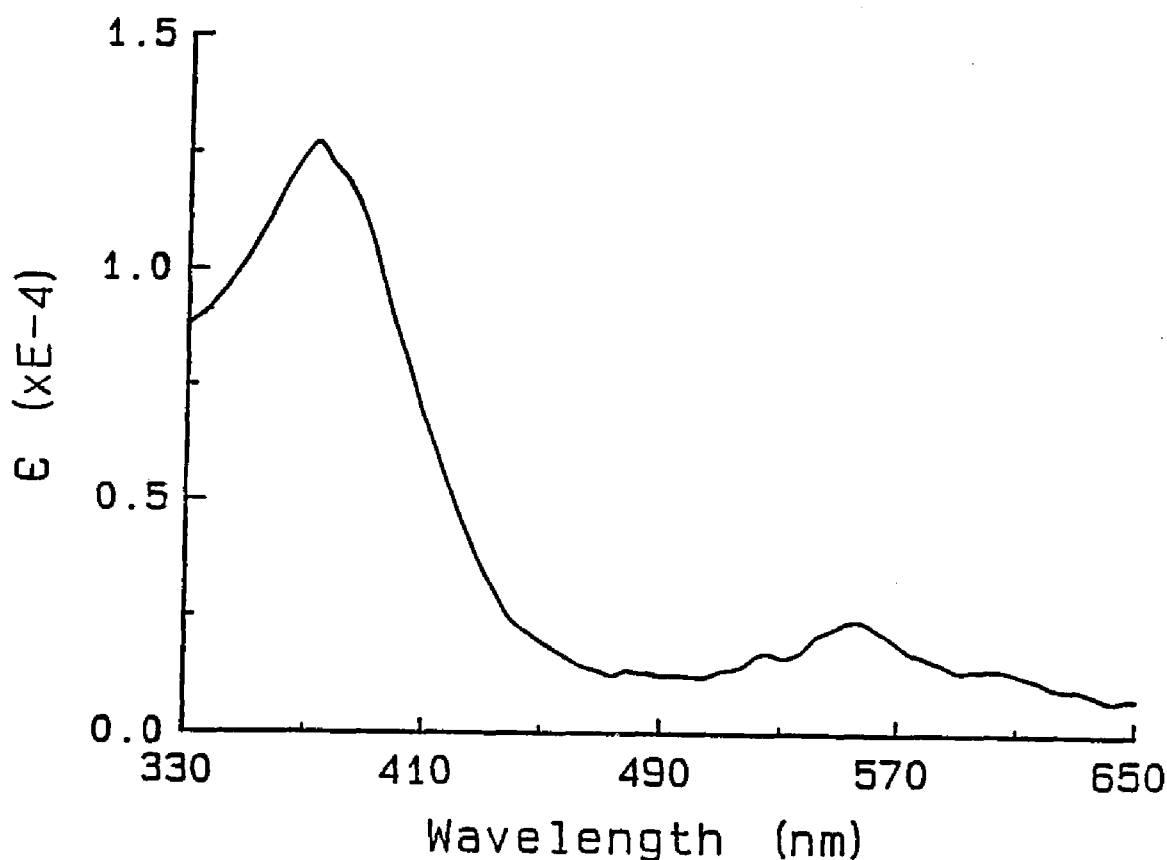


Figure 2.4: Difference spectrum of iron-free pentaammine ruthenium(III) histidine transferrin against apotransferrin from 330 nm to 650 nm. Conditions: 3.65 μM modified (6.03 residues) and native protein, pH 10.0. An intense band occurs at 377 nm and a broader, less intense band is found at 555 nm. The observed peaks are consistent with the pentaammine ruthenium-histidine trichloride model compound at pH 10.0. No change in the above spectrum is apparent after ultrafiltration or storage at 4°C, pH 7, for 6 weeks. FILES DS1, DS2 and DS3 Disk #3.

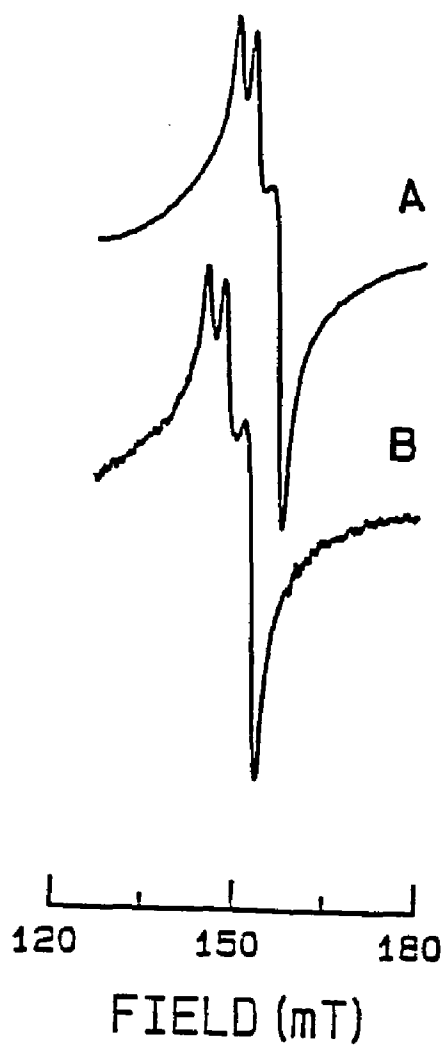


Figure 2.5: $g'=4.3$ EPR signals of diferric (~ 0.20 mM) (A) and 0.08 mM modified (1.46 His residues) (B) transferrin in 100 mM HEPES, pH 7.0 . Instrument settings are given in the Materials and Methods section.

Spectrophotometric titration at 295 nm of Fe(NTA)_2 into iron-free modified protein (2.0 His/mole) shows ruthenium modification did not affect the iron binding properties of transferrin at pH 7.5 (Figure 2.6). A clear break is seen at 2.05 moles Fe per mole of transferrin. Assuming two moles of iron bound to the protein, a prior assay at 280 nm indicates the molar absorptivity of the modified protein is 2.5% higher ($9.11 \times 10^4 \text{ M}^{-1}\text{cm}^{-1}$ at 280 nm) than the native value of $\epsilon_{280} = 8.89 \times 10^4 \text{ M}^{-1}\text{cm}^{-1}$.

The Iron Release Reaction

The semilogarithmic plot for absorbance vs. time data in the iron release reaction for native diferric and ruthenium modified transferrins (1.5 histidine residues) using pyrophosphate as the mediator is shown in Figure 2.7. The reaction is clearly biphasic at pH 7. The two macroscopic rate constants were extracted from the experimental curves using Equation 2.4 (Materials and Methods). The rate constants, k_N and k_C , obtained for modified protein were 0.060 min^{-1} and 0.013 min^{-1} . The values obtained for native protein under the same conditions were $k_N = 0.037 \text{ min}^{-1}$ and $k_C = 0.016 \text{ min}^{-1}$. In contrast to diferric transferrin modified with ethoxyformic anhydride, the rate of iron removal at the N-terminal site increases with increasing ruthenium modification. The rate of iron release from the C-terminal site is essentially unchanged at all degrees of

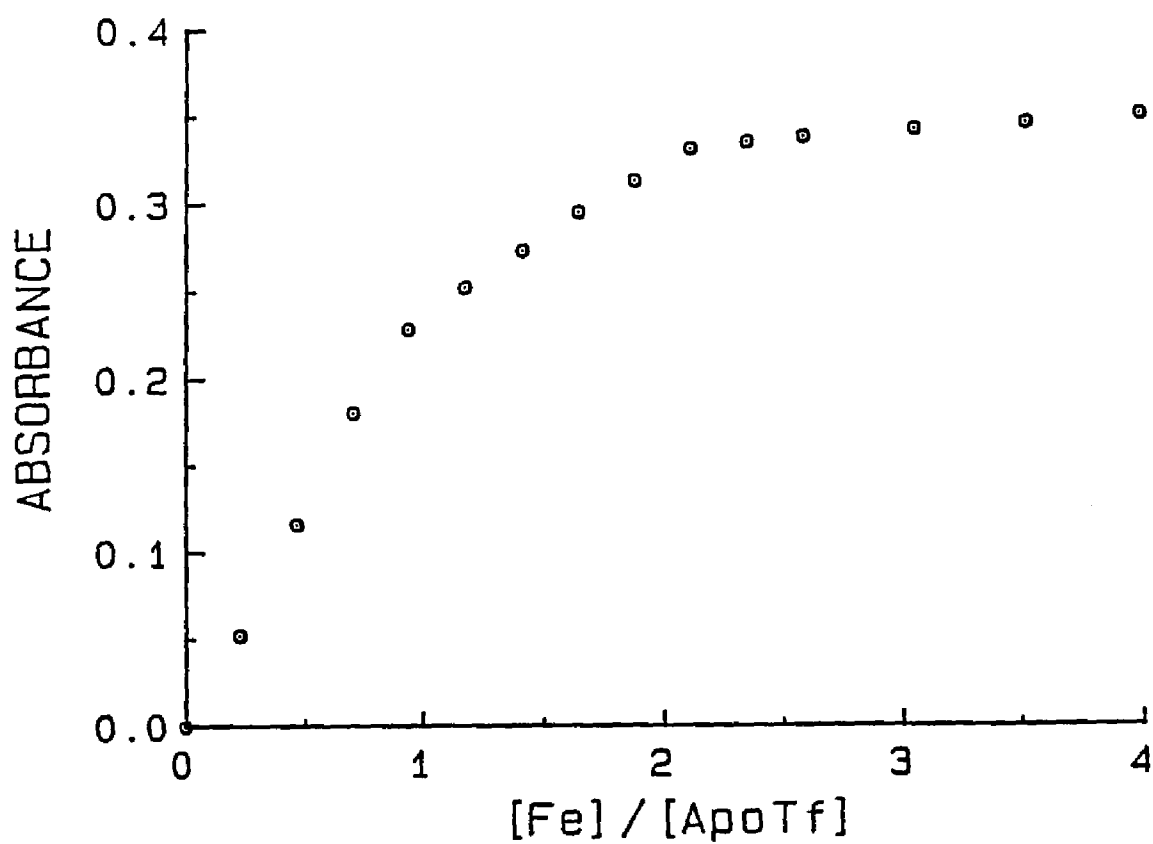


Figure 2.6: Titration of Fe(NTA)₂ into iron-free modified transferrin (2.0 His residues modified). Conditions: 20 μ M protein in 0.1 M HEPES, pH 7.5.

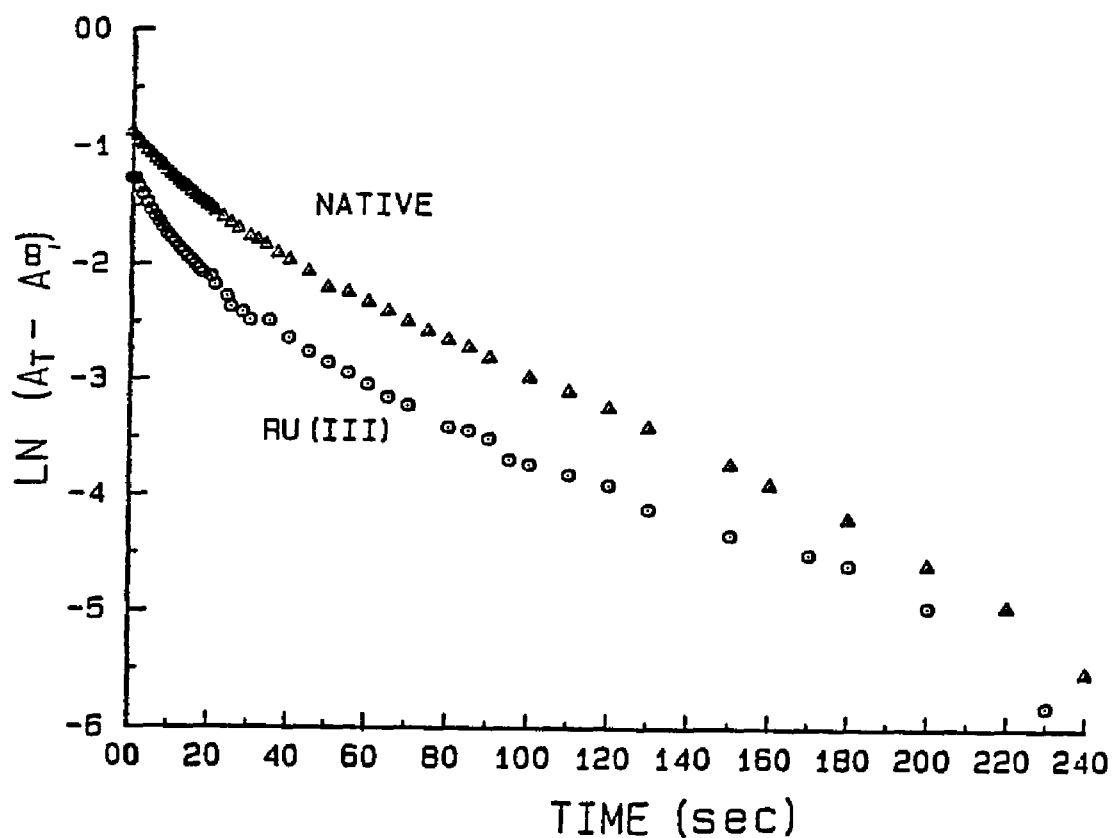


Figure 2.7: Semilogarithmic plot for absorbance data at 295 nm for the iron release reaction as a function of time at 25°C. Conditions: Δ - 17.8 μM native protein in 5 mM PPI, 0.10 M HEPES and 1.0 mM Des, pH 7.16. \circ - 17.0 μM two plots. The k_c values are the same for native and modified proteins. FILE: SPNAT, SPM2 Disk#3.

modification, however. Measurements were also made on native and modified C-terminal protein showing that the smaller rate constant was for the C-terminal site.

Iron release studies on a series of transferrins with varying degrees of ruthenium modification were carried out. The k_N rate constants extracted from the kinetic data are shown in the form of a Tsou Chen-Lu plot (Materials and Methods) in Figure 2.8. The activity parameter, a , is defined in terms of the macroscopic rate constants, k_u , k_p , and k_m for the unmodified, partially modified, and extensively modified protein, respectively ($a = (k_u - k_p) / (k_u - k_m)$). A linear plot results for $a^{1/i}$ vs. X when $i = 2$ and $i = 3$, whereas the data for $i = 1$ and $i = 4$ (not shown) are curved. The results imply that modification of two or three histidines is responsible for the increased kinetic stability of the protein with iron in the N-terminal site.

The F-test⁸⁷ as applied to the macroscopic rate constants obtained for the C-terminal site for five C-terminal monoferric transferrin samples (4 modified, 1 native) and seventeen diferric transferrin samples (14 modified, 3 native). In all cases k_C was not significantly different at a 95% confidence level implying that the C-terminal rate is unchanged upon modification.

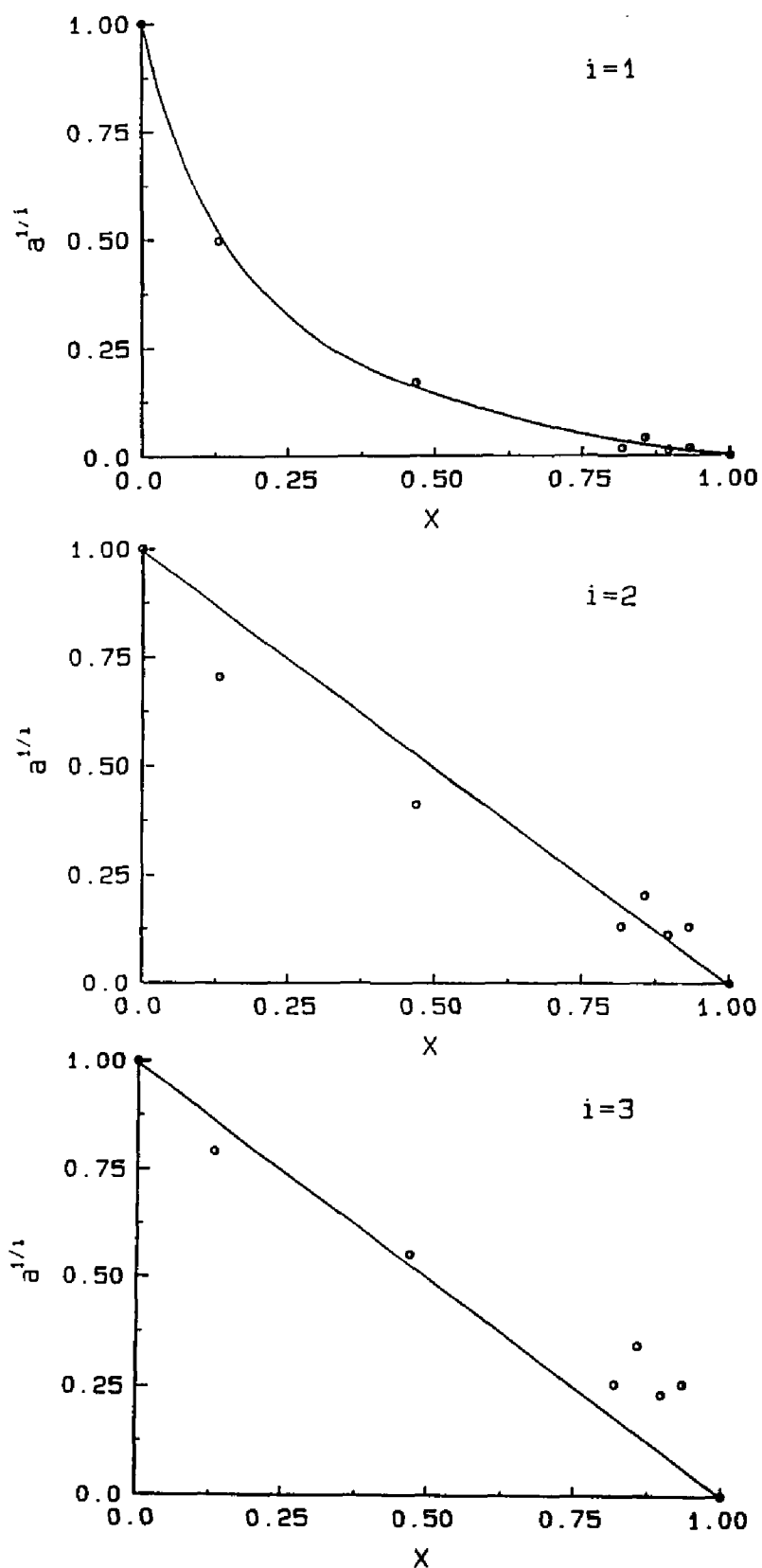


Figure 2.8: Tsou Chen-Lu plots for kinetic data for the N-terminal site for $i = 1$, $i = 2$ and $i = 3$. See Results section for definition of parameters.

DISCUSSION

The successful modification of histidine with aquopentaammine ruthenium(II) reagent to form stable pentaammine ruthenium-histidine complexes on diferric and C-terminal monoferric transferrin at neutral pH has been carried out. The reaction appears to be specific for histidines under the conditions described at reaction times up to 60 hours. Extensively modified protein consists of 6 modified histidine residues for diferric and 8 modified residues for C-terminal monoferric transferrin. The larger number of histidines modified in the monoferric protein is likely due to exposure of 2 histidines that are normally buried within the interior of the N-terminal lobe when iron is bound.

The electrostatic influence of the Ru(III) complex is probably responsible for the increase in rate of Fe release for the N-terminal site. The presence of octahedral $\text{Ru}(\text{NH}_3)_5\text{-His}$ may influence the local structure of the protein near the iron, resulting in a destabilization of the binding site. Another explanation is that the binding of mediators by the modified histidine is greatly enhanced due to the greater positive charge. Since the EPR spectrum shows that the iron binding site is essentially unaltered upon modification and titration of $\text{Fe}(\text{NTA})_2$ into modified protein shows that ruthenium incorporation does not inhibit iron binding, the second

possibility is the favored explanation.

The apparent linearity of $a^{1/i}$ vs. X for $i=2$ and $i=3$ show neither value can be excluded in determining the number of essential residues for the N-terminal site. More kinetic studies are needed to determine the i -value with certainty. In either case however, the value is in contrast with chemical modification of histidine using ethoxyformic anhydride where only one histidine was found to be essential. X-ray data for the N-terminal site indicate several surface-accessible histidines which makes either $i=2$ or $i=3$ a reasonable result. Also, the different modification reagents are likely to have had different effects on the Fe release kinetics (*i.e.* charge, sterics). The increase in k_N with no increase in k_C upon Ru(III) modification suggests the involvement of histidine residues which are not conserved in both domains. The X-ray diagram of lactoferrin shows HIS-26, HIS-276 and HIS-292 in the N-terminal lobe are on the protein surface and have no counterparts in the C-terminal domain. The corresponding residues in the N-terminal serum protein are HIS-25, HIS-273, and HIS-289. It is possible these residues are responsible for the observed kinetic effects. The presence of these non-conserved residues in the N-terminal site may also explain the observed kinetic stability of the C-site relative to the N-site in acidic media.

Further work is needed to determine the histidines which bind $\text{Ru}(\text{NH}_3)_5$. Such a study would involve the location of the modified histidines in the sequence by tryptic hydrolysis followed by HPLC of the peptide mixture. This method has been successful with low molecular weight proteins.^{62,64} High field NMR may also be used to determine which histidines are modified. The paramagnetism of the ruthenium(III) would likely have an effect on nearby proton and carbon nuclei analogous to lanthanide shift reagents.⁶⁶

CHAPTER III

ESTIMATION OF THE DISTANCE BETWEEN THE METAL
BINDING SITE AND HISTIDINE-Ru(III) COMPLEX
USING ENERGY TRANSFER FLUORESCENCE SPECTROSCOPY

INTRODUCTION

Distances in macromolecules can be measured by fluorescence energy transfer spectroscopy.⁷¹ In this study the distance from the iron binding site to neighboring histidines was determined using Ru(III) modified transferrin with terbium bound in the iron sites.

In the energy transfer experiment, the energy from an excited donor is transferred via a dipole-dipole, non-radiative mechanism to a second chromophore, the acceptor. The transfer between the two moieties can occur at distances up to 60 Å. Forsters' equations relate the efficiency of energy transfer to the spectral characteristics of the donor and acceptor, the relative orientation of their transition dipoles, and the distance between them.^{71,72}

$$E = 1 - (I/I_0) = 1 - (\tau/\tau_0) = [1 + (r/R_0)^6]^{-1} \quad (\text{Eq. 3.1})$$

Equation 3.1 shows that the efficiency of energy transfer, E , is related to the experimental fluorescence intensity, I , or fluorescence lifetime, τ , I_0 and τ_0 being the intensity and lifetime of the donor in the absence of an acceptor. E is inversely proportional to the sixth power of the donor-acceptor distance, r . R_0 is the Forster critical distance, the distance at which half of the excited donors are quenched by energy transfer to the acceptor. R_0 is a characteristic distance for every

donor-acceptor pair and can be expressed by Equation 3.2.

$$R_0^{1/6} \text{ (cm)} = 8.78 \times 10^{-25} (\kappa^2 \eta^{-4} \Phi J) \quad (\text{Eq. 3.2})$$

where κ^2 is the dipole-dipole orientation factor, η is the index of refraction of the intervening medium, Φ is the fluorescence quantum yield of the donor in the absence of energy transfer and J is the value of the overlap integral. J is a measure of the degree of overlap between the absorption spectrum of the acceptor and the fluorescence emission spectrum of the donor. The overlap integral is given by Equation 3.3.

$$J = \frac{\int F(\lambda) \epsilon(\lambda) \lambda^4 d\lambda}{\int F(\lambda) d\lambda} \quad (\text{cm}^3 \text{M}^{-1}) \quad (\text{Eq. 3.3})$$

where $F(\lambda)$ is the fluorescence intensity (in arbitrary units) of the energy donor at wavelength λ (in cm), and $\epsilon(\lambda)$ is the molar absorptivity (in $\text{M}^{-1} \text{cm}^{-1}$) of the acceptor.

The validity of the above equations has been demonstrated using well defined model systems.^{73,74} Figure 3.1 describes the system under study. Terbium(III) bound

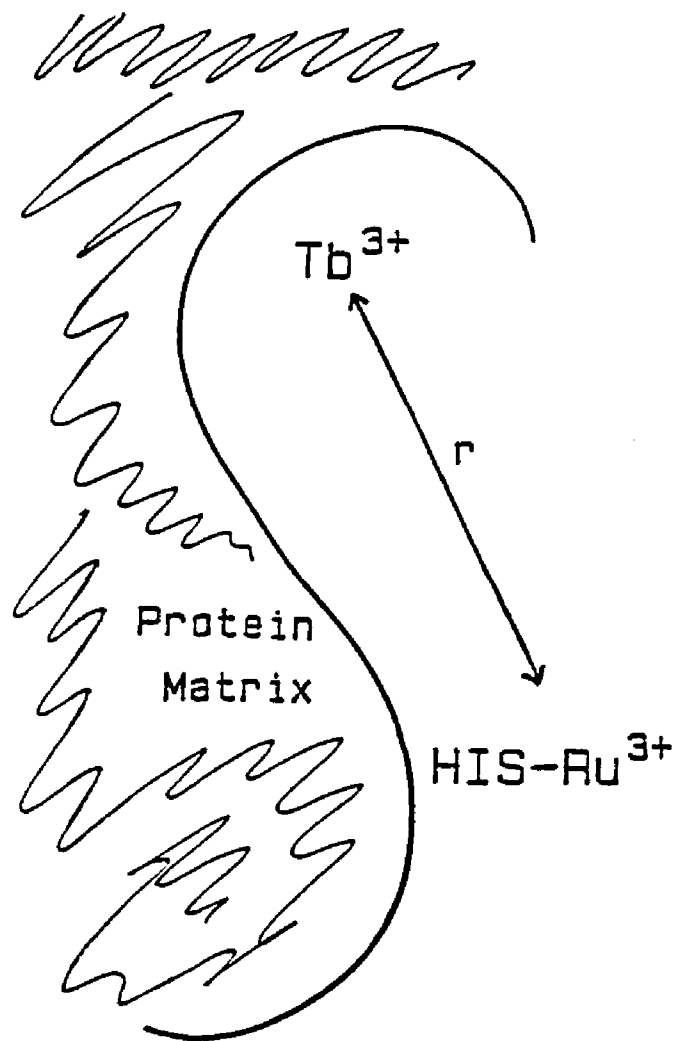


Figure 3.1: Representation of energy transfer between a bound terbium ion (donor) and a nearby Ru(III)-histidine complex (acceptor) for one of the transferrin binding sites. Transfer of energy from donor to acceptor results in fluorescence quenching of donor emission. The efficiency of energy transfer is proportional to the inverse sixth power of the distance, r , between the donor and acceptor.

to transferrin is the donor and the $\text{Ru}(\text{NH}_3)_5\text{-His}$ complex is the acceptor chromophore. The possibility that two or more $\text{Ru}(\text{NH}_3)_5\text{-His}$ molecules close enough to participate in energy transfer from the excited terbium cannot be excluded. If parallel first order kinetics for energy transfer from the donor to several acceptors is assumed, the transfer efficiency for N acceptors is given by Equation 3.4.

$$E(N) = \frac{\sum (R_0/r_i)^6}{1 + \sum (R_0/r_i)^6} \quad (\text{Eq. 3.4})$$

where r_i is the distance from the donor to the i^{th} acceptor, the sum is over N pairs, and R_0 is assumed to be the same for all donor-acceptor pairs.⁷⁵

Lanthanide(III) ions such as Tb(III) are distinguished among metallic cations in their ability to fluoresce in solution at room temperature.⁷⁶ For terbium complexes in aqueous solution, essentially all emission emanates from the $^5\text{D}_4$ state when the excitation energy is less than at 480 nm.⁷⁷ The lowest energy multiplets associated with the $4f^8$ electronic configuration are shown in Figure 3.2.

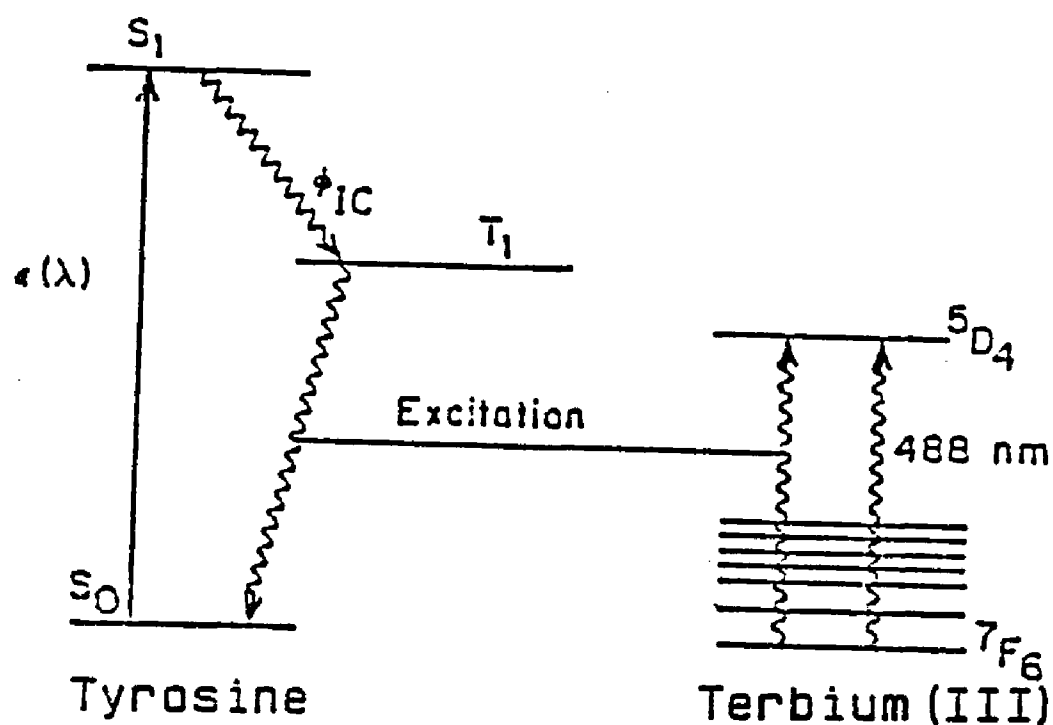


Figure 3.2: Fluorescence emission emanates from the $5D_4$ excited state of Tb(III) in diterbium transferrin. Direct excitation occurs by absorption of 488 nm light using an argon laser. The $5D_4$ state can also be populated indirectly by excitation of the aromatic ring in tyrosine to the S_1 level followed by $S_1 \rightarrow T_1$ transition. Relaxation energy to the bound terbium. ¹Adapted from reference 83.

The terbium ion can be excited with a 488 nm argon ion laser. The input intensity of a laser is required due the low molar absorptivity, $\epsilon_{488} = 0.005 \text{ M}^{-1}\text{cm}^{-1}$. Alternatively, the $^5\text{D}_4$ state can be populated indirectly by uv excitation of an adjacent aromatic group such as a coordinated tyrosine in transferrin, followed by intramolecular energy transfer to terbium shown in Figure 3.2.⁷⁸ Since the molar absorptivity is relatively large ($\epsilon_{295} = 10^3 \text{ M}^{-1}\text{cm}^{-1}$), a xenon arc source is suitable for energy transfer measurements using indirect excitation.

Energy transfer has been used to probe the distance between the two metal ions in transferrin by observing Tb^{3+} at one site and Fe^{3+} or Mn^{3+} at the other site.⁷⁹ Yeh and Meares used fluorescence energy transfer to examine the distance of closest approach between metals attached to transferrin and freely diffusing Tb^{3+} chelate complexes in solution.⁷⁸

Diterbium transferrin has been characterized using uv difference absorbance and fluorescence spectroscopy.^{14,79,80} The potential use of terbium transferrin as a label for the immunoassay for gentamicin has also been studied.⁸¹

Recent studies suggest that previous data on terbium binding to transferrin may have been misinterpreted.⁸² Harris has shown that bicarbonate interferes with terbium binding, apparently due to the formation of lanthanide carbonate complexes.⁸² Previous energy transfer studies

using terbium were done with 5 - 25 mM bicarbonate.^{14,79,80} When no bicarbonate was added, an increase in binding capacity was observed for lanthanide metals.⁸²

MATERIALS AND METHODS

Precautions were taken to avoid trace metal ion impurities. Clean labware was soaked in 6 M HCl followed by rinsing with doubly distilled deionized water. Good Buffers were chosen for their lack of contamination by heavy metals.⁸⁴ Reagent solutions were stored over Chelex 100. The supernatant was carefully decanted before use. Protein solutions were centrifuged just prior to experimentation to remove trace particles which might interfere with fluorescence measurements. Chemicals were reagent grade and obtained from the following sources.

TbCl₃ - Aldrich

CAPS (3-[Cyclohexylamino]-1-propanesulfonic acid)
- Sigma

Tetraethyl Rhodamine B - K & K Laboratories

Native and Modified Transferrin

Iron-free native transferrin was prepared and assayed as described in Chapter I. C-terminal and diferric transferrin were modified with aquopentaammine ruthenium(II) and subsequently made iron-free using protocols described in Chapter II.

In an attempt to deactivate N-terminal histidine ligands, ruthenium-modified C-terminal transferrin was further modified with ethoxyformic anhydride (EFA). In this procedure, EFA was added in 1 - 5 μ L increments to a stirring solution of 4.6 - 4.9 μ M C-terminal protein in

0.10 M HEPES, pH 7.3, to make a final concentration of 1.2×10^{-3} M in EFA. The extent of modification was monitored by uv-difference spectroscopy at 242 nm using ruthenium-modified C-terminal protein as the reference. The solution was then ultrafiltered using an Amicon cell fitted with a PM30 membrane. The volume was replaced three times (90% V/V per change) with 0.010 M HEPES, pH 7.3, and the protein concentrated and frozen until use.

Fluorescence Studies

Fluorescence work was initially performed using a Perkin-Elmer 204 spectrophotometer equipped with a Xenon-arc excitation source. The instrument has a rotary turret which can accommodate up to four cuvettes per experiment. Unless otherwise stated, fluorescence measurements were made at room temperature with an excitation wavelength of 295 nm.

To determine the effect of aqueous terbium fluorescence on terbium fluorescence bound to native protein, aliquots of 1.5×10^{-4} M TbCl_3 were added to 3 mL of 2 μM native transferrin in 0.050 M HEPES, pH 7.5, to 100% saturate the protein. The same volume of TbCl_3 was titrated into a blank solution containing 0.050 M HEPES. The emission spectrum was scanned from 460 - 650 nm. It was determined that the fluorescence intensity contribution of aqueous terbium was negligible at the sensitivity setting used for terbium transferrin.

A pH study was performed to determine the pH range where two moles terbium bind quantitatively per mole of native or modified transferrin. A series of 2.0 μM native or modified proteins were prepared in 0.050 M HEPES, pH 8 or pH 9, and 0.050 M CAPS (3-[Cyclohexylamino]-1-propanesulfonic acid), pH 10.0. Terbium chloride (1.5×10^{-4} M) was added in 10 μL aliquots to 3.0 mL of protein and the increase in emission intensity was monitored at 544 nm until equilibration occurred (5 - 40 min depending upon the sample). Native transferrin binds two moles of terbium quantitatively at pH 7.0, 8.0 and 10.0. Modified transferrin binds quantitatively only at pH 10.0 however. Therefore, all subsequent fluorescence studies were made at pH 10.0.

A Beer's law plot determined the concentration range where fluorescence intensity was linearly proportional to the concentration. The linear range was 0.5 μM - 3.0 μM and 2.0 μM - 6.0 μM for native and modified transferrin respectively.

Terbium Titrations

Iron-free native and modified transferrin stock solutions were diluted to 0.50 - 2.0 μM and 2.0 - 6.0 μM respectively with 0.010 M HEPES, pH 7.0. The exact concentration was determined spectrophotometrically using $\epsilon_{280\text{nm}} = 8.89 \times 10^4 \text{ M}^{-1}\text{cm}^{-1}$. Solid CAPS buffer was added to the solution to make a final concentration of 0.050 M

in buffer. The pH was then adjusted to 10.0 using dilute NH_3 .

The proteins (3.0 mL) were titrated with 10 - 20 μL aliquots of 1.5×10^{-4} M TbCl_3 and fluorescence was monitored at 544 nm or 487 nm. When aliquots were added to fluorescence cuvettes, the solution was carefully mixed with a fire-polished pipette. The shutter to the sample was closed between titration readings to prevent photodegradation. Typical equilibration time was 20 minutes for modified samples. Native apotransferrin (0.50 or 1.0 μM) was always titrated in conjunction with three modified protein samples in order to determine instrumental variations between runs. Each fluorescence measurement was taken at different sensitivities (X10S4 - X10S9) to obtain maximum signal on the chart.

Overlap Integral

The emission spectrum used to evaluate the overlap integral was obtained using IL-SLM 8000 fluorescence spectrophotometer with Xe-arc as the excitation source. Native transferrin (2.0 μM in 0.050 M CAPS, pH 10) was titrated with terbium and a series of emission spectra were obtained from 450 nm to 650 nm. The instrumental parameters are listed in Table IV.

The absorption spectrum of the Ru(III) -His-transferrin complex (3.56 μM in 0.010 M CAPS,

Table IV

IL-SLM 8000 Instrumental Parameters
Using Xenon Arc Excitation

excitation λ	= 295 nm
lower λ limit	= 450 nm
upper λ limit	= 650 nm
bandwidth excitation monochrometer	= 2.0 nm
bandwidth emission monochrometer	= 12.0 nm
wavelength increment	= 0.25 nm
Acquisition Time	= 10 s
Acquisition Time (detector)	= 0.1 s
Channel Number	= A
Photomultiplier Voltage (coarse)	= 1.0 kV
Photomultiplier Voltage (fine)	= + 45 to 51 V
Sensitivity	= 100

pH 10.0) from 670 - 300 nm was obtained by difference spectroscopy using native apoprotein at the same concentration in the reference cell. Variations in wavelength ($\sim 3\text{nm}$) between the CARY 219A absorbance and IL-SLMB000 fluorescence measurements were corrected with a standard solution of rhodamine B (tetraethyl rhodamine; 2.9×10^{-7} M in ethanol) which has excitation and emission peaks at 541 nm and 580 nm respectively.⁸⁵ A computer program using trapezoidal quadrature equations in increments of 1.0 and 2.0 nm was used to evaluate the overlap integral.

The Tsou Chen Lu statistical method was employed to determine the number of histidine residues involved in the fluorescence quenching of transferrin modified with pentaammine ruthenium. The extent of Ru modification was determined by atomic emission as described in Chapter II.

RESULTS

When terbium is bound to transferrin the fluorescence intensity is greatly enhanced. The fluorescence emission spectra from 450 - 650 nm of terbium in water and in transferrin (4.0×10^{-5} M Tb) are shown in Figure 3.3. The emission intensity of aqueous terbium has been amplified 5000 times in order to compare its spectral shape with terbium transferrin (100% saturated). The three peaks for aqueous terbium occur at 481, 537 and 582 nm. The binding of terbium to the protein led to bathochromic spectral shifts occurring at 487, 544, 583 nm and the appearance of a small peak at 620 nm. The most striking contrast between the two spectra is the appearance of a doublet at 487 nm. This shows that terbium indeed binds in two different environments leading to two resolvable transitions. These observations are consistent with previous studies.^{14,78,80}

Native transferrin (20 μ M) in 0.10 M HEPES, pH 8.9, was titrated with Tb^{3+} . The increase in fluorescence intensity was monitored at 487 nm and 544 nm simultaneously. The titration curves are shown in Figure 3.4 for both wavelengths. Fluorescence intensity rose sharply as terbium was initially bound to transferrin, continued to increase more gradually after the addition of 1.5 moles of Tb per mole of protein and leveled off at 2.0 Tb per mole of transferrin.

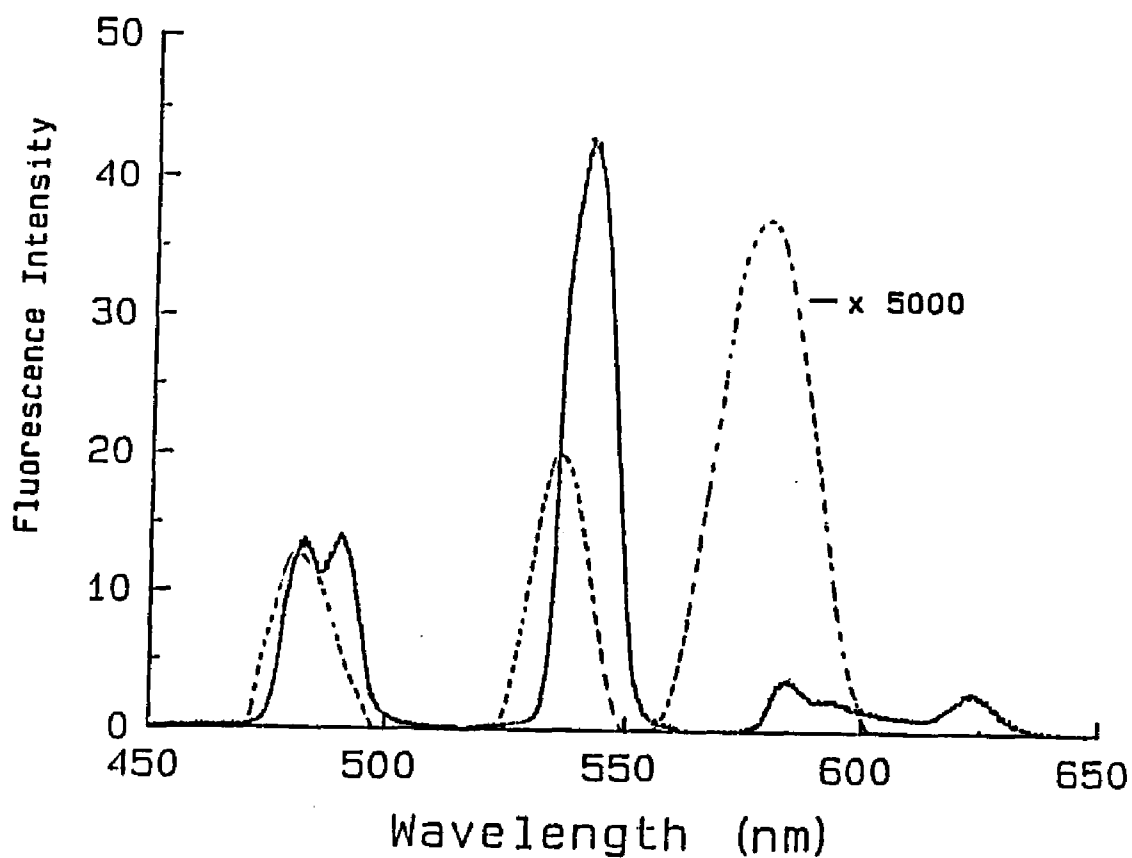


Figure 3.3: The fluorescence emission intensity of aqueous Tb(III)(dashed line), and Tb-transferrin 100% saturated (solid line). Conditions: 4.0×10^{-5} M Tb(III) in unbuffered aqueous solution and in 20 μ M transferrin in 0.050 M HEPES, pH 8.5. The emission intensity of the aqueous terbium has been amplified 5000 times in order to compare the two spectra on the same plot. FILE: TBH20, TBTf, Disk #3.

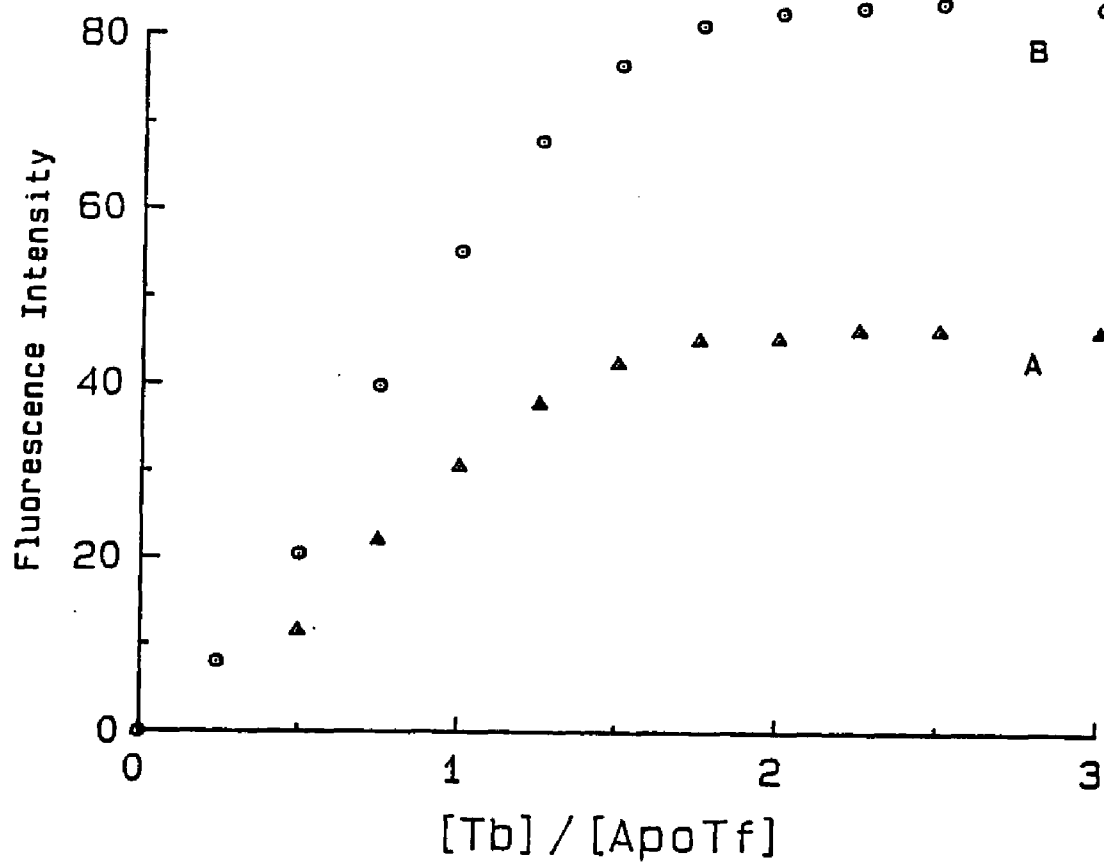


Figure 3.4: Titration of native transferrin with Tb(III). Conditions: 20 μ M apotransferrin in 0.10 M HEPES, pH 8.9. The emission intensity is shown at 487 nm (A) and 544 nm (B) as a function of the amount of terbium. FILE: TB487, TB544, Disk# 2

The maxima at 544 nm was chosen for use in energy transfer measurements due to its greater emission intensity. In subsequent experiments native transferrin was shown to bind 2 moles of terbium per mole of protein in the pH range 7 - 10.

The degree of binding as a function of pH for ruthenium modified transferrin (5.5 His residues modified) is shown in Figure 3.5. When transferrin was titrated at pH 8, the fluorescence intensity increased until 1.2 moles of Tb were added per mole of transferrin. Further addition of terbium led to a decrease in signal. This effect was observed for all modified proteins at pH 8 and 9. In all cases, the binding of 2 moles of terbium occurred at pH 10.

Fluorescence quenching due to modification with ruthenium is illustrated by titration curves in Figure 3.6 for native and modified transferrin (3.8 and 6.0 His residues). The fluorescence intensities of the modified proteins were amplified four-fold in order to be observed on the same plot. The modified proteins bound 1.8 - 2.0 moles of terbium at pH 10, showing that ruthenium modification did not inhibit binding. The degree of quenching, or reduced energy transfer efficiency was 80, and 98.3% for 3.8 and 6.0 modified residues, respectively.

Fluorescence studies of transferrin modified to varying degrees with pentaammine ruthenium are shown in Figure 3.7 in the form of a Tsou Chen-Lu plot. In this study, I is the fluorescence intensity and X is the mole fraction of

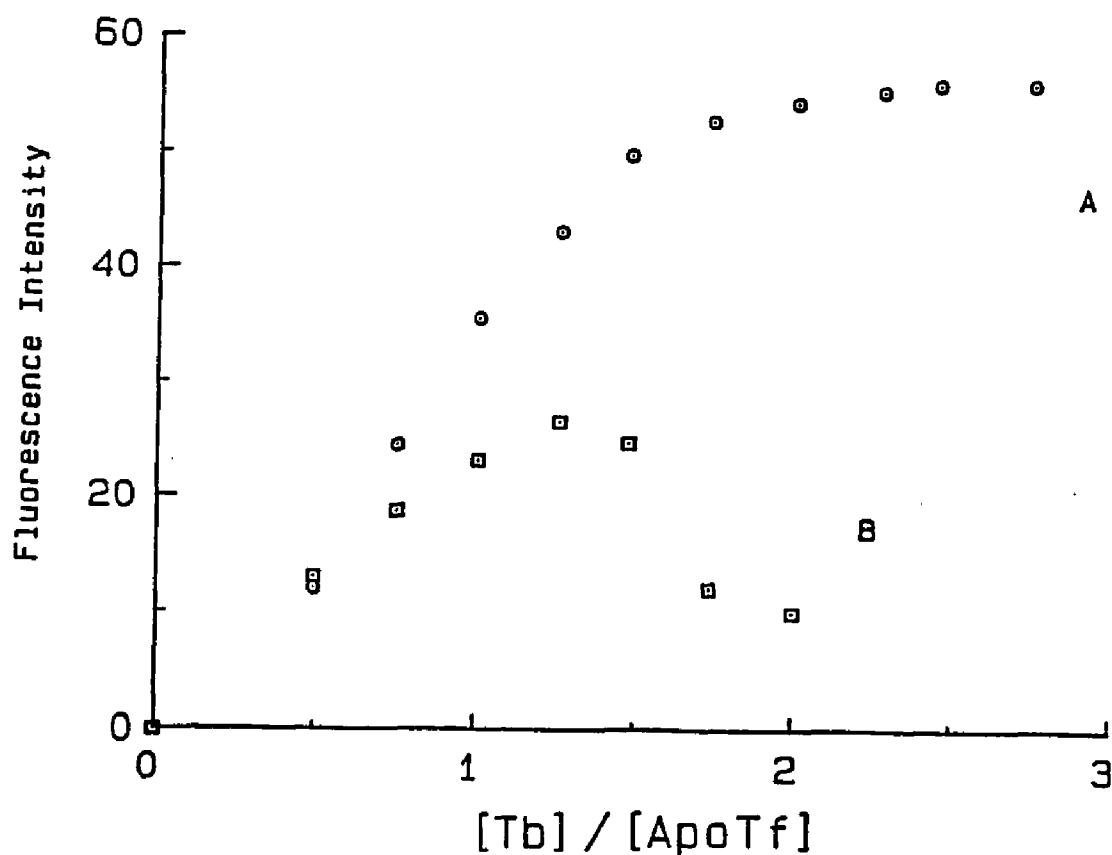


Figure 3.5: Terbium titration into modified protein (5.5 residues modified). Curve A, 2.0 μ M protein in 0.050 M CAPS, pH 10. Curve B, 2.0 μ M protein in 0.050 M HEPES, pH 8. Binding of 2 moles of terbium occurs at pH 10 (see Results). FILE: TBM38, TBM310, Disk#3.

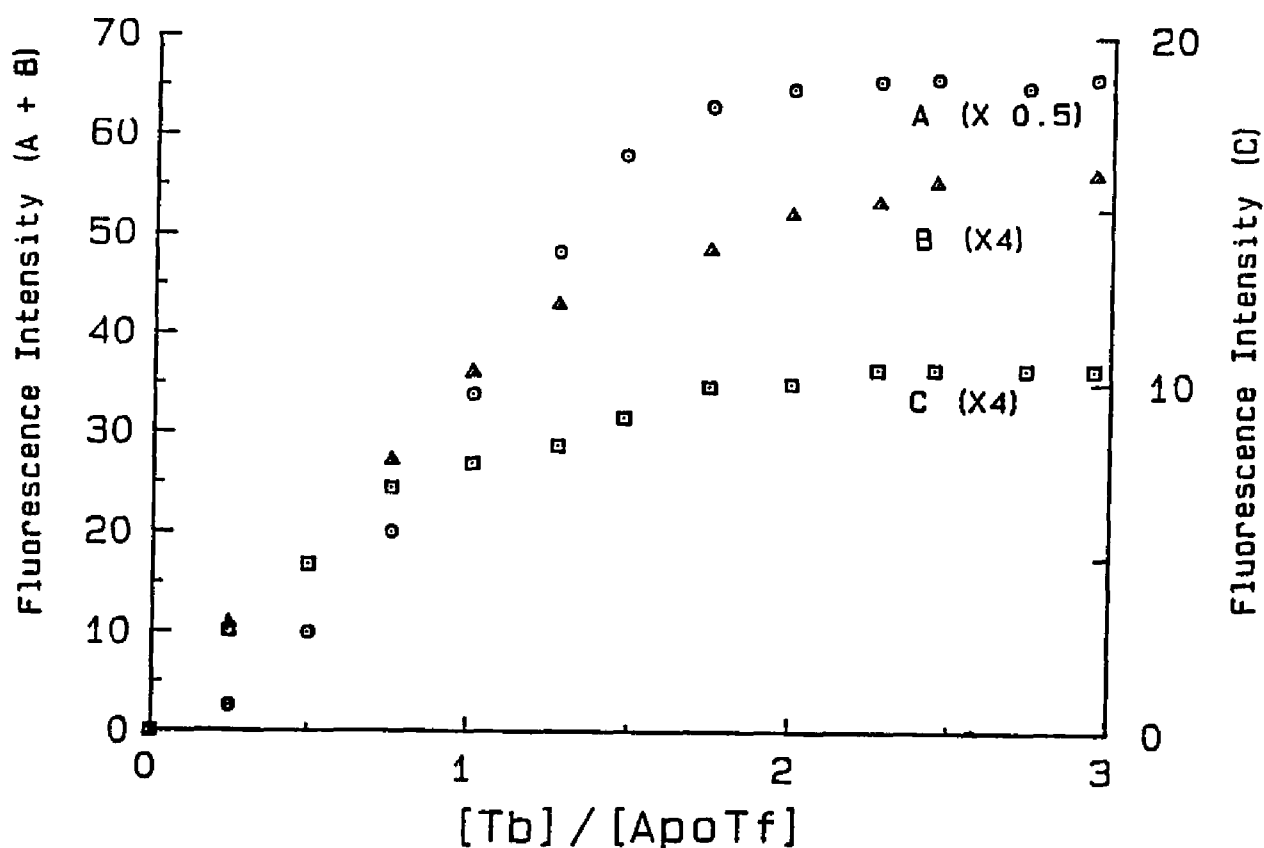


Figure 3.6: Titration curves for native (A), 3.8 residues modified (B) and 6.0 residues modified (C). The emission intensity for the modified proteins have been amplified by a factor of 4 and that of the native attenuated by a factor of 2 in order to display the curves on the same plot. The y-axis on the right refers to extensively modified transferrin (\square). Conditions: 1.9 - 2.1 μ M proteins in 0.050 M CAPS, pH 10.0. The degree of quenching is 80% and 98.3% for 3.8 and 6.0 modified histidine residues respectively. FILE: A) M0B4, B) M2B4, C) M4B4 Disk #2.

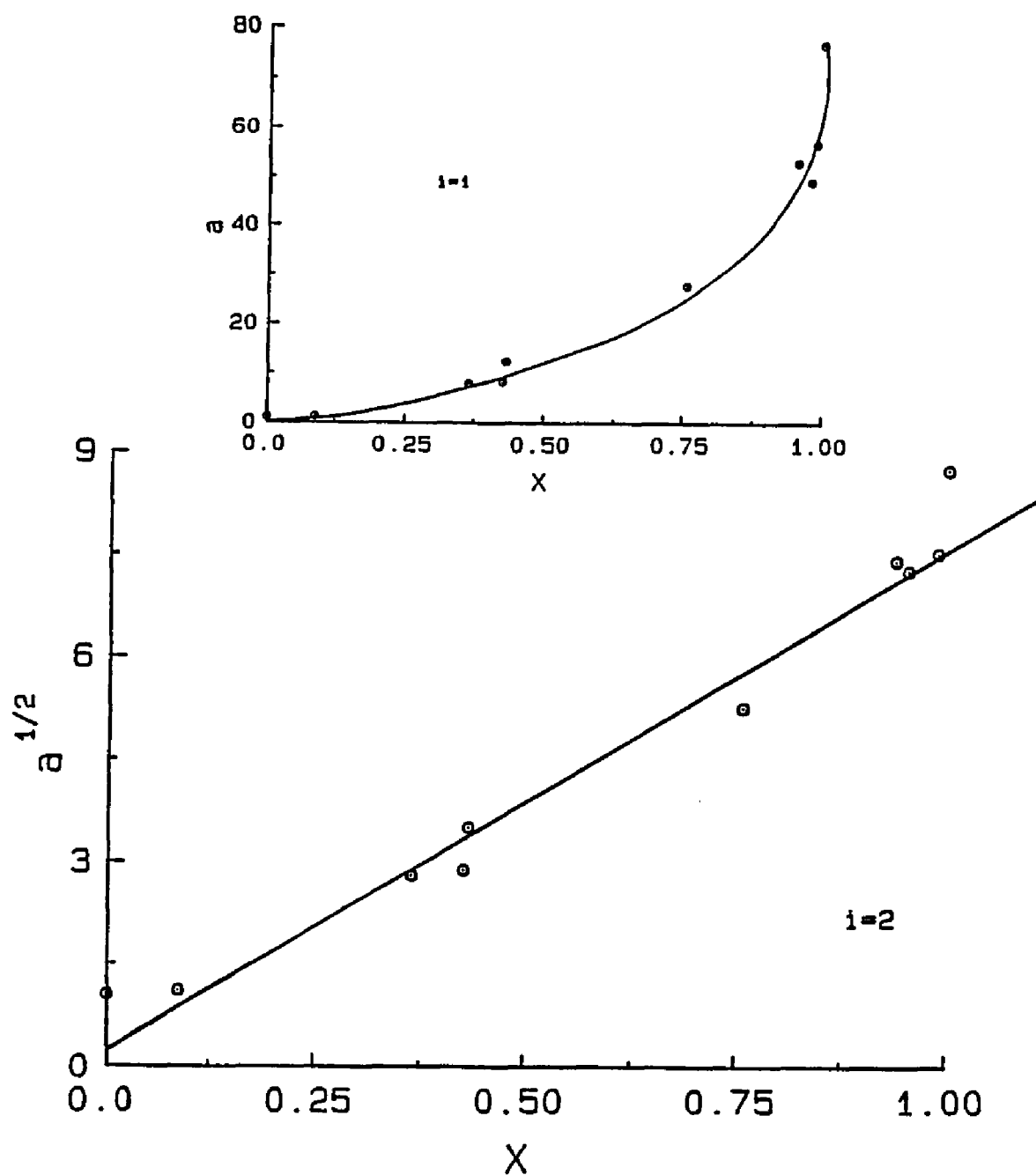


Figure 3.7: Tsou Chen-Lu plot for $i = 2$ and $i = 1$ (inset). A linear plot for $i = 2$ suggests that 2 histidines are responsible for fluorescence quenching (see Results).

modified residues in a pool of six equally reactive histidines. A linear plot is obtained when $i = 2$, implying that two histidines are principally responsible for the fluorescence quenching observed.

The Forster critical distance R_0 is directly proportional to J , n^{-4} , Φ , and κ^2 . Of these terms only the overlap integral J can be measured experimentally. The degree of spectral overlap is shown in Figure 3.8 for the fluorescence emission of diterbium transferrin and the ruthenium absorption spectrum as iron-free modified transferrin (6.0 His residues modified). The spectra have been corrected for wavelength variations between the two instruments. The overlap integral from 450 - 650 nm was evaluated to be $2.81 \times 10^{-15} \text{ M}^{-1} \text{ cm}^{-1}$ using Equation 3.3. The factor κ^2 is a measure of the angular dependence between the transition dipoles of the donor and acceptor. A value for κ^2 can range from 0 to 4. In this study, the isotropic value of $2/3$ was used. This assumes that the donor and acceptor rotate freely in a time that is short compared to the excited state lifetime of the donor, a situation normally obtained with Tb(III)-protein complexes.

The quantum yield, Φ , for Tb-transferrin cannot be directly measured due to its low molar absorptivity at 488 nm ($\epsilon \sim 10^{-3} \text{ M}^{-1} \text{ cm}^{-1}$). Upper and lower limits of 0.25 and 0.68 have been estimated by O'Hara and coworkers using lifetime measurements. Recommended values for the index

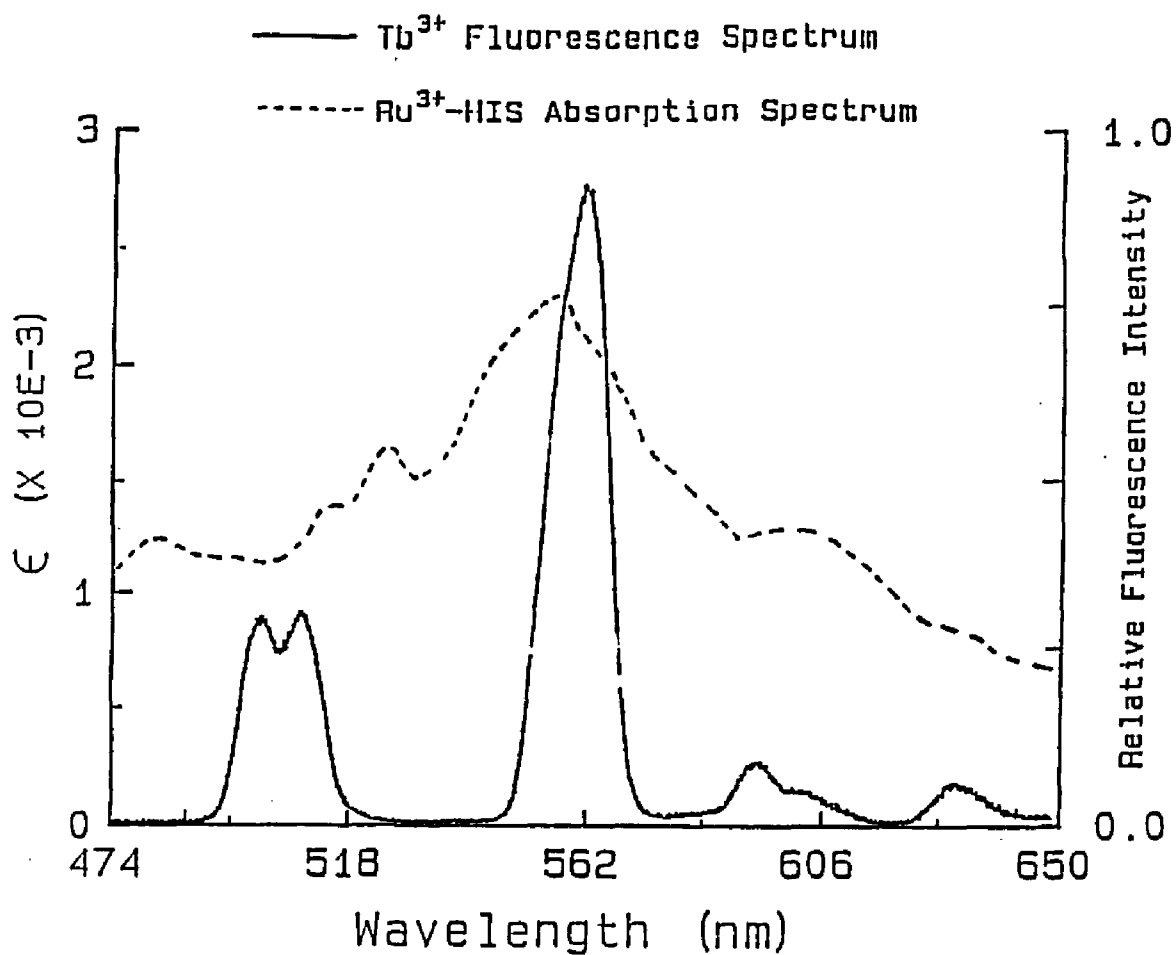


Figure 3.8: Degree of spectral overlap for the Tb-transferrin emission spectrum (A) and the pentaammine ruthenium-histidine absorption spectrum (B). The overlap integral was evaluated to be $2.81 \times 10^{-15} \text{ M}^{-1} \text{ cm}^3$ by Equation 3.3.

of refraction, n , for protein solutions are 1.33 - 1.50.⁸⁶

The maximum degree of quenching for the extensively modified protein (6.8 His residues) occurred where $I/I_0 = 0.017$. Using the upper and lower limits for n and Φ_D , the distance was calculated to be between 1.14 nm and 1.25 nm with corresponding R_0 values between 2.25 nm and 2.46 nm. The results from the Tsou Chen-Lu plot indicate that two histidines are contributing to energy transfer. The distance, using Equation 3.4 with $N = 2$, thus becomes 1.32 nm to 1.42 nm. This calculation assumes that energy transfer follows parallel first order kinetics with R_0 being the same for both donor acceptor pairs.

An attempt to totally deactivate the N-terminal site prior to fluorescence energy transfer measurements by ethoxyformylating C-terminal transferrin which had been previously modified with pentaammine ruthenium was not successful. A comparison of the histidine residues Ru modified before and after ethoxyformylation showed that EFA displaced some ruthenium histidine residues. Upon modification with EFA, partially modified C-terminal transferrin, (7.0 residues) the amount of ruthenium contained on the protein decreased to 2.8 residues modified. For 8.1 Ru(III) residues modified the amount decreased to 3.45 when the protein was treated with EFA. In addition, fluorescence titration studies on doubly modified transferrins indicated binding of ~ 2 moles Tb.

DISCUSSION

Preliminary fluorescence experiments reveal interesting features of the binding of terbium to transferrin. In particular, the binding chemistry appears to change when ruthenium is incorporated into the protein. The titration curve for terbium binding to native transferrin in the pH range 7.0 - 8.5 shows two breaks at ~ 1.2 and 2.0 moles of added terbium, indicating the stepwise binding of the metal to the protein (Figure 3.4). In contrast, ruthenium(III) modification inhibits the binding of two moles of Tb(III) at pH values less than 10. For example, Figure 3.5 shows the initial binding of terbium to one site at pH 8. As the titration progresses, however, the fluorescence intensity decreases. The incorporation of Ru(III) may render the binding region too positively charged for complete Tb(III) binding at pH values lower than 10. When the same titration is carried out at pH 10, the ruthenium modified protein binds two moles of terbium, implicating the deprotonation of tyrosines and/or lysines residues ($pK_a \sim 10$) in the binding of the metal.

EPR and optical measurements at pH 10 indicate that dithorium and divanadyl transferrins undergo a "C- to N-conformational change" making the C-terminal binding site

spectroscopically identical to the N-terminal site. Additional experiments are needed to determine the type of conformational transition occurring at pH 10. The titration data of modified transferrins suggests equivalent binding affinities in the two sites for Tb(III) at pH 10 since two separate breaks are not observed (Figure 3.6). This observation is consistent with a conformational transition at pH 10.

The results from energy transfer studies of proteins extensively modified with ruthenium(III) indicate the donor-acceptor distance is between 1.14 nm and 1.25 nm using the upper and lower values for η and Φ (see Results). If two histidines are responsible for energy transfer as implicated by the Tsou-Chen Lu method, the range becomes 1.32 nm to 1.44 nm. The actual distance is probably smaller than calculated here since the protein is incompletely modified.

For exact calculations, the R_0 for each acceptor should be considered separately, by measuring the degree of fluorescence quenching and evaluating the overlap integral for each donor acceptor pair. Gennis and Cantor have performed exact energy transfer calculations for one donor and multiple acceptors, treating each R_0 independently.⁷⁵ The results differed by 15% from the assumed value showing that Equation 3.4 is acceptable for semi-quantitative measurements.

The amino acid sequence data for human serum transferrin shows there are four histidines conserved in both domains. By viewing the stereodiagram of the α -carbons of the lactoferrin structure, the distance between these histidines and the metal site can be estimated. The following designations are numbered according to sequence of serum transferrin. The distance between α -carbons in an α -helix is taken as 0.15 nm. Histidines-119, HIS-207, and HIS-242 in the N-terminal domain and their counterparts in the C-domain, are within the calculated upper limit of 14.4Å. Histidine-119 and HIS-242 are approximately the same distance to the metal. From the stereodiagram HIS-119 is seen to be partially buried by helical strands, making it the least likely to form the pentaammine ruthenium-HIS complex. Histidine-242 is a surface accessible residue. Histidine-207 is the closest to the metal site and is positioned between TYR-188 and TYR-95 protein ligands. Like HIS-242, HIS-207 is also surface accessible.

In conclusion, histidine residues not coordinated to the metal are very likely involved in the iron release reaction. Histidines 207 and 545 are strong candidates. However these assignments were based on the lactoferrin structure and slight differences in amino acid sequencing could lead to different positioning of histidines in human serum transferrin. These assignments are based on an X-ray structure and may not reflect the dynamics present in solution.

Possible future work should include separation of partially modified proteins via cation exchange chromatography. This would permit isolation of the two histidines so that an exact R_0 can be determined for each residue. The determination of the quantum yield would reduce the uncertainty values in the distance (An error of 0.2 in ϕ leads to an error of 8.3% in R_0). An indirect method for measuring the quantum yield of terbium transferrin using model compounds has been suggested by Meares.⁷⁸

CONCLUSION

The differences in rates of iron release using EFA and pentaammineruthenium(II) chemical modification reagents point toward a possible dual role for non-coordinated histidines in transferrin. Previous studies in this laboratory have implicated a single histidine near the metal in each domain is involved in the iron release mechanism. In contrast, this study suggests two non-conserved histidines in the N-terminal site are involved. Pentaammineruthenium(II) is known to react appreciably with only surface accessible residues whereas EFA is probably small enough to diffuse into the interior near the binding site. The X-ray structure shows that many of the surface accessible histidines are contained in the outer coils of α -helixes (Figure 3.9). One possible function of these histidines is to stabilize the conformational folding of the protein by hydrogen bonding to other amino acids. When histidine is not protonated, both nitrogens can act as either a donor or acceptor of hydrogen bonding. Upon ionization however, histidine loses this amphiprotic property possibly destabilizing other amino acids and triggering a conformational change. Examination of the structure also shows non-conserved histidines present only in the N-terminal lobe may explain some of the differences between the acid lability of the

N-terminal site as well as the marked increase in rate of iron release from the N-site upon modification with the ruthenium(III) reagent.

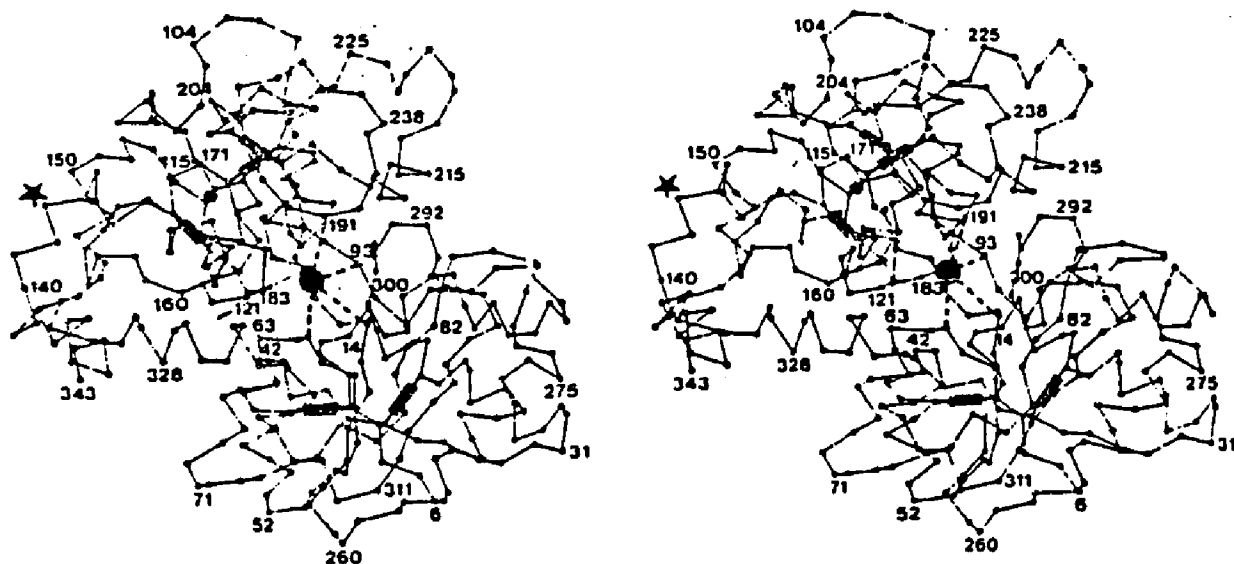


Figure 3.9: Stereodigram of the α -carbons in the X-ray structure of lactoferrin. Adapted from reference 20.

REFERENCE LIST

REFERENCES

1. Morgan, E.H. Molec. Aspects Med. 1981, 4, 1 - 123.
2. Spiro, Th.G.; Saltman, P. Struct. Bonding 1969, 6, 116-156.
3. Crichton, R.R. Struct. Bonding 1973, 17, 67 - 134.
4. Fletcher, J.; Huehns, E.R. Nature 1968, 218, 1211.
5. Palmour, R.M.; Sutton, H.E. Biochemistry 1971, 10, 4026- 4032.
6. Aisen, P.; Listowski, I. Ann. Rev. Biochem. 1980, 49, 357.
7. Chasteen, N.D. Coord. Chem. Rev. 1977, 22, 1.
8. Brines, R.D.; Brock, J.H. Biochem. Biophys. 1983, 75 229 - 235.
9. Custer, M.C.; Hansen, J.N. Appl. Environmental Microbio. 1983, 45, 942 - 945.
10. Baldwin, D.A.; Jenny, E.R.; Aisen, P. J. Biol. Chem. 1984, 259, 13391-13394.
11. Tan, A.T.; Woodworth, R.C. Biochemistry 1969, 8, 3711 3716.
12. Harris, D.C.; Aisen, P. In Proteins of Iron Storage and Transport Crichton, R.R., Ed.; Elsevier: Amsterdam, 1975, pp. 59 - 66.
13. Gelb, M.H.; Harris, D.C. Arch. Biochem. Biophys. 1980 200, 93 - 98.
14. Luk, C.K. Biochemistry 1971, 10, 2828 - 2843.
15. Williams, J.; Grace, S.A.; Williams, J.M. Biochem. J. 1982 201, 417-419.
16. Aisen, P.; Leibman, A.; Zweier, J.L. J. Biol. Chem. 1978, 253, 1930.
17. Octave, J-N.; Schneider, Y-J.; Crichton, R.R.; Trouet, A. Eur. J. Biochem. 1981, 115, 611 - 618.
18. Octave, J-N.; Schneider, Y-J.; Trouet, A.; Crichton, R.R. Trends Biochem. Sci. 1983, 8, 217 - 220.

19. Newman, R.; Schneider, C.; Sutherland, R.;
Vodinelich L.; Greaves, M. Trends Biochem. Sci. 1982
397-400.
20. Anderson, B.F.; Baker, H.M.; Dodson, E.J.;
Norris, ; G.E Rumball, S.V.; Waters, J.M.; Baker,
E.N. Proc. Nat'l Acad. Sci. USA 1987, 84, 1769 -
1773.
21. Williams, J. Biochem. J. 1982, 201, 647 - 651.
22. Recorara, V.L.; Harris, W.R.; Carrano, C.J.; Raymond,
K.N. Biochemistry 1981, 20, 7033 - 7034.
23. Alsaadi, B.M.; Williams, R.J.P.; Woodworth, R.C. J.
Inorg. Biochem. 981, 15, 1 - 10.
24. Rogers, T.B.; Gold, B.A.; Feeney, R.E. Biochemistry
1977, 16, 2299 - 2305.
25. Chasteen, N.D. Trends Biochem. Sci. 1983, 8, 272 -
275.
26. Morgan, E.H. Biochim. Biophys. Acta. 1979, 580, 312
326.
27. Najarian, R.C.; Harris, D.C.; Aisen, P. J. Biol.
Chem 1978, 253, 38 - 42.
28. Zak, O.; Aisen, P. Biochim. Biophys. Acta. 1983,
742 490 - 495.
29. Cowart, R.E.; Kojima, N.; Bates, G.W. J. Biol. Chem.
1982, 257, 7560.
30. Cowart, R.E.; Swope S.; Lok, T.T.; Chasteen, N.D.;
Bates, G.W. J. Biol. Chem. 1986, 261, 4607 - 4614.
31. Price, E.M.; Gibson, J. J. Biol. Chem. 1972, 247,
8031.
32. Baldwin, D.A.; deSousa, D.M.R. Biochem. Biophys.
Res Commun. 1981, 99, 1101.
33. Chasteen, N.D.; Thompson, C.P.; Martin, D.M. In The
Release of Iron from Transferrin. An Overview.
Xavier, A Ed.; VCH: West Germany, 1986 ; pp. 278 -
286.
34. Chasteen, N.D.; Williams, J. Biochem. J. 1981, 193,
717 - 727.
35. Thompson, C.P.; Grady, J.K.; Chasteen, N.D. J. Biol.
Chem. 1986, 261, 13128-13134.

36. Morgan, E.H. Biochim. Biophys. Acta 1977, 499, 169 -177.
37. Delaney, T.A.; Morgan, W.H.; Morgan, E.H. Biochim. Biophys. Acta 1982, 701, 295 - 304.
38. Morgan, E.H. Biochim. Biophys. Acta 1979, 580, 312 326.
39. ibid Reference 17.
40. Patterson, S.; Morgan, E.H. J. Cell. Physiol. 1980 105, 489 - 502.
41. Thompson, C.P. Ph.D. Dissertation, University of New Hampshire, Durham, N.H. 1985, pp.1-91.
42. Thompson, C.P.; Chasteen, N.D.; Martin, D.M. Rev. Port Quim. 1985, 27, 119-120.
43. Folajtar, D.A. A Study of the Thermodynamics of Anion Binding to Human Serum Transferrin. Ph.D. Thesis, Univ. of New Hampshire, Durham, NH (1982).
44. Ovadi, J.; Liubor, S.; Elodi, P. Acta Biochem. Biophys Acad. Sci. Hung. 1967, 2, 455.
45. Carver, F.J.; Frieden, E. J. Biol. Chem. 1978, 17, 1 - 172.
46. Pollack, S.; Vanderhoff, G.; Lasky, F. Biochim. Biophys. Acta. 1977, 497, 481 - 487.
47. Bartlett, G.R. Biochem. Biophys. Res. Comm. 1976 70, 1055.
48. Bartlett, G.R. Biochem. Biophys. Res. Comm. 1976 70, 1063.
49. Goucher, C.R.; Taylor, J.F. J. Biol. Chem. 1964 239, 2251.
50. Clarke, M.J. J. Amer. Chem. Soc. 1978, 100, 5068 -5075 and references therein.
51. Clark, M.J.; Buchbinder, M. Inorg. Chim. Acta 1978, 7, L87-L88.
52. Matthews, C.R.; Erickson, P.M.; Froebe, C.L. Biochim. Biophys. Acta 1980, 624, 499-510.
53. Yocom, K.M.; Winkler, D.G.; Bordignon, E.; Gray, H.B. Chem. Scripta 1983, 21, 29-33.

54. Margalit, R.; Pecht, I.; Gray, H.B. J. Am. Chem. Soc. 1982, 105,
55. Crutchley, R.J.; Ellis Jr., W.R.; Gray, H.B. J. Am. Chem. Soc. 1985, 107, 5002-5004.
56. Kostic, N.M.; Margalit, R.; Che, C-M.; Gray, H.B. J. Am. Chem. Soc. 1983, 105, 7765-7767.
57. Nocera, D.G.; Winkler, J.R.; Yocom, K.M.; Bordignon, Gray, H.B. J. Am. Chem. Soc. 1984, 106, 5145-5150.
58. Che, C-M.; Margalit, R.; Chiang, H-J.; Gray, H.B. Inorg. Chim. Acta 1987, 135, 33-35.
59. Sundberg, R.J.; Gupta, G. Bioinorg. Chem. 1973, 3, 39-48.
60. Ford, P.C. Coord. Chem. Rev. 1970, 5, 75-99.
61. Matthews, C.R.; Erickson, P.M.; Van Vliet, D.L.; Petersheim J. Am. Chem. Soc. 1978, 100, 2260-2266.
62. Recchia, J.; Matthews, C.R.; Rhee, M-J.; Horrocks Jr. W.D. Biochem. Biophys. Acta 1982, 702, 105-111.
63. Yocom, K.M.; Shelton, J.B.; Shelton, J.R.; Schroeder, W.A.; ,Worosila, G.; Isied, S.S.; Bordington, E.; Gray, H Proc. Natl. Acad. Sci. USA 1982, 79, 7052-7055.
64. Margalit, R.; Kostic, N.M.; Che, C-M.; Blair, D.F.; Chiang, H-j.; Pecht, I.; Shelton, J.B.; Shelton, J.R.; Schroeder, W.A.; Gray, H.B. Proc. Natl. Acad. Sci. USA 1984, 81, 6554-6558.
65. Marglit, R.; Pecht, I.; Gray, H.B. J. Am. Chem. Soc. 1983, 105, 301-302.
66. Matthews, C.R.; Recchia, J.; Froebe, C.L. Anal. Biochem 1981, 112, 329 - 337.
67. Maron, S.H. Fundamentals of Physical Chemistry (1974), Macmillan Publishing Co., New York. p 575.
68. Sotera, J.J., Atomic Absorption Methods Manual (1979), Instrumentation Laboratories, Wilmington, MA.
69. Tsou,C-L. Scientia Sinica 1962 11, 1535-1557.
70. Kuehn, C.G.; Taube, H. J. Am. Chem. Soc. 1976, 98, 689.

71. Forster, T. Ann. Physik. 1948, 2, 55 - 75.
72. Stryer, L. Ann. Rev. Biochem. 1978, 47, 819 - 846.
73. Haugland, R.P.; Yguerabide, J.; Stryer, L. Proc. Nat. Acad. Sci. USA 1969, 63, 23.
74. Latt, S.A.; Cheung, H.T.; Blout, E.R. J. Amer. Chem. Soc. 1965, 87, 995.
75. Gennis, R.B.; Cantor, C.R. J. Biol. Chem. 1972, 1, 2509 - 2517.
76. Horrocks, W.DeW.; Sudnick, D.R. Acc. Chem. Res. 198 14, 384 - 392.
77. Richardson, F.S. Chem. Rev. 1982, 82, 541 - 552.
78. Yeh, S.M.; Meares, C.F. J. Biol. Chem. 1980, 19, 5057 - 5062.
79. O'Hara, P.; Yeh, S.M.; Meares, C.F.; Bersohn, R. J. Biol. Chem. 1981, 20, 4704 - 4708.
80. Meares, C.F.; Ledbetter, J.E. J. Biol. Chem. 1978, 16, 5178 - 5180.
81. Wilmott, N.J.; Miller, J.N.; Tyson, J.F. Analyst 1984, 109, 343 - 345.
82. Harris, W.R. Inorg. Chem. 1986, 25, 2041 - 2045.
84. Ferguson, W.J.; Good, N.E. Anal. Biochem. 1980, 104, 300.
85. Miller, J.N. Standards in Fluorescence Spectrometry (1981), Chapman and Hall, New York.
86. R.T.A. MacGillivray,; Mendez, E.; Shewale J.G.; Sinha, S.K.; J. Lineback-Zins; K. Brew J. Biol. Chem. 1983, 258, 3543-3553.
87. Schenk, G.H.; Hahn, R.B.; Hartkopf, A.V. Quantitative Analytical Chemistry (1977), Allyn and Bacon, Boston.